STYRELSEN FÖR

VINTERSJÖFARTSFORSKNING

WINTER NAVIGATION RESEARCH BOARD

Research Report No 139

Shayan Rabizade, Tommi Mikkola, Mikko Suominen

OPEN WATER EMISSIONS RELATED TO ICE CLASS

Finnish Transport and Communications Agency
Finnish Transport Infrastructure Agency
Finland

Swedish Maritime Administration
Swedish Transport Agency
Sweden

Talvimerenkulun tutkimusraportit — Winter Navigation Research Reports
ISSN 2342-4303
ISBN 978-952-425-025-2

FOREWORD

In this report no 139, the Winter Navigation Research Board presents the results of OWERIC - Open water emissions related to ice class. Project goal was to estimate the effects of ice class on the efficiency of a vessel when compared to similar open water designed vessels especially considering EEDI.

The Winter Navigation Research Board warmly thanks the author for this report.

Helsinki

April 2026

Ville Häyrynen

Finnish Transport and Communications Agency

Amund Lindberg

Swedish Maritime Administration

Helena Orädd

Finnish Transport Infrastructure Agency

Jonas Gustaffson

Swedish Transport Agency

Open Water Emissions Related to Ice Class (OWERIC)

Department of Mechanical Engineering
School of Engineering
Aalto University
Espoo, Finland

Shayan Rabizade, Tommi Mikkola, Mikko Suominen

Author(s)	Shayan Rabizade, Tommi Mikkola, Mikko Suominen		
Title	Open Water Emissions Related to Ice Class [OWERIC]		
Version Control	Original Manuscript		
Date	25.03.2026	**Number of pages** 37	**Language** English

Abstract

Ships navigating in ice require structural reinforcement, which significantly af- fects their performance and efficiency in open-water conditions. This study inves- tigates the impact of ice strengthening on the Energy Efficiency Design Index (EEDI) by considering two scenarios: fixed deadweight and fixed displacement. A series of bulk carriers were analyzed, incorporating additional steel weight and machinery weight changes associated with ice-class requirements. The results show that ice strengthening leads to increased displacement or reduced capacity, both resulting in higher Attained EEDI. When accounting for added weight, the analysis indicates that its effect is better represented through changes in hull di- mensions, particularly length and block coefficient, which increase resistance and power demand. The findings further reveal that the resulting EEDI increase is not proportional to the correction factors currently specified in regulations, suggest- ing that these factors may underestimate the performance penalty of ice-class ships. Eventually, the operation in icy waters impose significant disparities between Finnish-Swedish Ice Class Rules (FSICR) power requirements and EEDI regulations, as ice-class strengthening (e.g., thicker propeller blades) and ice-optimized hull forms increase resistance, reduce hydrodynamic efficiency, and ultimately demand higher installed power despite reduced transport capacity.

Keywords Energy Efficiency Design Index, Ice-going Ship, Ship Lightweight, Power Requirements, Ice-Going Propeller

Contents

1 Introduction **4**

2 Methodology **5**

2.1 Energy Efficiency Design Index (EEDI) 5

2.2 Correction Factors 6

2.2.1 Capacity Factor [f_i] 6

2.2.2 Power Correction Factor (f_j) 8

2.3 Developed Method 9

2.3.1 Estimation of Lightweight 11

2.3.2 Estimation of Added Weight 13

2.3.3 Impact of Lightweight Increase on Ship Dimensions Under Fixed Deadweight 15

2.3.4 Impact of Lightweight Increase on Ship Dimensions Under Fixed Displacement 16

2.3.5 Estimation of Propulsive Power 16

2.3.6 Estimation of Increase in EEDI 18

3 Result **19**

3.1 EEDI Changes: Capacity Correction with Extra Steel Weight 19

3.1.1 Fixed Displacement without Dimensional Changes 19

3.1.2 Fixed Displacement with Dimensional Changes 20

3.1.3 Fixed Deadweight with Increase in Length 20

3.1.4 Fixed Deadweight with Increase in Length and Reduction in C_b 22

3.1.5 Comparison of Attained EEDI 22

3.2 EEDI Changes: Capacity Correction with Extra Steel and Machinery Weight . 24

3.2.1 Fixed Displacement without Dimensional Changes 24

3.2.2 Fixed Displacement with Dimensional Changes 25

3.2.3 Fixed Deadweight with Increase in Length 25

3.2.4 Fixed Deadweight with Increase in Length and Reduction in C_b 26

3.2.5 Comparison of Attained EEDI 26

3.3 Minimum Engine Power 28

3.4 Effect of Thicker Propeller Blade 28

3.5 Effect energy saving technologies [f_m] 29

3.5.1 Bulbous bow 30

3.5.2 Ice Going bow 30

4 Discussion **31**

5 Conclusion **32**

Nomenclature

Table 1: Nomenclature and definitions of symbols used in the study.

Symbol	Description
B	Breadth of the ship [m]
C_b	Block coefficient
C_F	Frictional resistance coefficient
C_m	Machinery coefficient
C_o	Outfit coefficient
DWT	Deadweight [tons]
$EEDI$	Energy Efficiency Design Index
$FSICR$	Finnish-Swedish Ice Class Rules
f_i	Capacity correction factor
f_{iVSE}	ship-specific voluntary structural enhancement correction factor
f_{j0}	Preliminary calculated power correction factor
$f_{j,\min}$	Minimum required power correction factor
H_s	Superstructure height [m]
IC	Ice-class condition
L	Length of the ship [m]
L_{LW}	Length of the waterline at full load [m]
L_{PP}	Length between perpendiculars [m]
LWT	Lightweight [tons]
MCR	Maximum continuous rating of power [kW]
ME	Main Engine
OW	Open-water condition
P_E	Engine power [MW]
$P_{aver,\ \text{ow(DWT)}}$	Average power of open-water (DWT) [MW]
$P_{\text{installed}}$	Installed power of the ice-class ship [MW]
R_T	Total resistance [N]
Re	Reynolds number
$RES(L)$	Residual function for determining ship length [m]
S	Wetted surface area [m^2]
T	Draft of the ship [m]
V	Ship speed [m/s]
W_I	Increase in lightweight due to ice strengthening [tons]
W_M	Machinery weight [tons]
W_O	Outfitting weight [tons]
W_{St}	Steel structure weight [tons]
Δ	Displacement [tons]
α	Fractional increase in lightweight from ice strengthening
β	Ratio of displacement to lightweight
ε	Tolerance for convergence criteria in numerical methods
μ	Dynamic viscosity of water [Pa·s]
ρ	Density of water [kg/m^3]

1 Introduction

Ships operating in ice-covered waters are subjected to unique environmental conditions that impose significant structural and propulsion requirements. In regions such as the Baltic Sea, where sea ice persists from late autumn to early spring, vessels must be designed to withstand ice-induced loads while maintaining safe and reliable operation. This is particularly critical for countries like Finland, where more than 95% of imports and exports are transported by sea, making maritime transportation essential for both economic activity and security of supply [1]. However, interactions between sea ice and the ship hull generate substantial global and local loads that challenge the structural integrity of the vessel. To ensure safe operation, ships are reinforced through thicker hull plating and additional structural members, while propulsion systems are strengthened to maintain maneuverability in ice-covered conditions. Although these measures improve resistance to ice-induced loads, they also increase the vessel's lightweight and propulsion power requirements, which can negatively affect open-water performance and overall transportation efficiency.

Previous studies have shown that ice-class requirements significantly increase the structural weight of ships. For example, Alanko [22] demonstrated that compliance with Finnish–Swedish ice class rules increases hull steel weight by approximately 1–10% for ships in different ice classes. These standards, originally developed for vessels operating in the Baltic Sea, have influenced ice-class regulations worldwide. Higher ice classes, particularly those intended for Arctic operations, typically require substantially greater structural reinforcement [19]. Similarly, Avellan [17] investigated the influence of structural design choices on hull steel weight and showed that ice-class upgrades can significantly increase structural mass, particularly due to thicker shell plating and reduced frame spacing. More recently, Blasig [13] analyzed the effect of ice class selection on lightweight variations, demonstrating that reducing the ice class from IA Super to IC may decrease the total steel weight by approximately 1.57%. However, such reductions may lead to operational limitations, including an increased risk of vessel immobilization during severe ice conditions. A systematic comparison between open-water vessels and ice-going ships was conducted by Aker Arctic [14], showing that ice-strengthening leads to both increased lightweight and higher installed propulsion power.

In parallel with structural considerations, environmental regulations have introduced new constraints on ship design. In 2011, the Marine Environment Protection Committee (MEPC) of the International Maritime Organization introduced the Energy Efficiency Design Index (EEDI) under MARPOL Annex VI to reduce CO_2 emissions from ships. The regulatory framework was later expanded to include the Energy Efficiency Existing Ship Index (EEXI) and the Carbon Intensity Indicator (CII) [2, 3]. These regulations aim to improve transportation efficiency by limiting installed propulsion power relative to transport capacity. However, vessels designed for ice navigation typically require increased propulsion power to maintain safe operation in ice-covered waters, which may complicate compliance with these efficiency regulations.

Although previous studies have quantified the structural weight increase associated with ice strengthening, the influence of ice-class requirements on the open-water performance of ships remains insufficiently understood. In particular, the combined effects of increased lightweight and propulsion requirements on compliance with the EEDI framework have received limited attention. This study investigates how ice-class requirements influence the open-water performance of a representative vessel, with a particular focus on changes in lightweight and power demand under the EEDI framework. To achieve this, the effects of structural reinforcement and increased propulsion power are evaluated using two analytical approaches: a fixed displacement method and a fixed deadweight method.

The analysis is conducted using reference ship data presented in Table 15. Methods for estimating the changes in lightweight and propulsion power are described in Secs. 2. The resulting impacts on EEDI capacity and power demand are analyzed using both fixed displacement and fixed deadweight approaches, followed by the implications of bow design and propeller characteristics for ice-going vessels in Sec. 3. Finally, the study concludes with a discussion and concluding remarks in Secs. 4 and 5 respectively.

2 Methodology

This section presents the methodology used to evaluate the impact of ice-class requirements on ship performance. First, the Energy Efficiency Design Index (EEDI) framework is introduced based on the relevant regulatory guidelines [4]. Next, correction factors proposed in the literature [14] are applied to estimate variations in transport capacity and propulsion power between ice-going and open-water vessels. Building on these elements, a systematic approach is developed to quantify how ice-class modifications influence the performance of a reference ship originally designed for open-water conditions.

2.1 Energy Efficiency Design Index (EEDI)

This study evaluates ship performance using the Energy Efficiency Design Index (EEDI), which is defined by regulations for vessels built and delivered since 2015 [4]. The EEDI quantifies carbon emissions relative to transport work by relating propulsion power and capacity to the resulting CO_2 output. In this framework, the Attained EEDI must remain below the Required EEDI, which is determined from a regulatory reference line. The mathematical formulation of these parameters is given in Eqs. 1 and 2, forming the basis for the performance assessment used in this study.

$$\text{Required EEDI} = (1 - \frac{X}{100}) \cdot \text{Reference line} \tag{1}$$

$$\text{Attained EEDI} = \frac{CE_{ME} + CE_{AE} + CE_{PTI} - CE_{IEET}}{f_{correction} \cdot DWT \cdot V_{ref}} \tag{2}$$

Here, X (%) denotes the reduction factor required to improve energy efficiency relative to the reference line, which is established using statistical regression based on ship data, typically as a function of vessel capacity [4]. In Eq. 2, the terms CE_{ME}, CE_{AE}, and CE_{PTI} represent the CO_2 emissions from the main engines, auxiliary engines, and power take-in systems, respectively. In contrast, CE_{IEET} accounts for emission reductions achieved through innovative energy-efficient technologies. Furthermore, the denominator represents transport work by combining deadweight tonnage (DWT) and reference speed (V_{ref}). The correction factor $f_{correction}$ accounts for differences between open-water and ice-class vessels, particularly in terms of propulsion power and capacity [5]. The more detailed version of Eq. 2 is presented in

Eq. 3.

$$\frac{\left(\prod_{j=1}^{n} f_j\right) \times \left(\sum_{i=1}^{n^{\mathrm{ME}}} P_{\mathrm{ME}(i)}\, C_{\mathrm{FME}(i)}\, \mathrm{SFC}_{\mathrm{ME}(i)} + P_{AE}\, C_{FAE}\, \mathrm{SFC}^{*}_{AE}\right)}{f_i\, \mathrm{DWT}\, f_w\, V_{\mathrm{ref}}}$$

$$+ \frac{\left(\prod_{j=1}^{n} f_j\right) \times \left(\sum_{i=1}^{n^{\mathrm{PTI}}} P_{\mathrm{PTI}(i)} - \sum_{i=1}^{n^{\mathrm{eff}}} f_{\mathrm{eff}(i)}\, P_{AE_{\mathrm{eff}(i)}}\right) C_{FAE}\, \mathrm{SFC}_{AE}}{f_i\, \mathrm{DWT}\, f_w\, V_{\mathrm{ref}}} \tag{3}$$

$$- \frac{\sum_{i=1}^{n^{\mathrm{eff}}} f_{\mathrm{eff}(i)}\, P_{\mathrm{eff}(i)}\, C_{FME}\, \mathrm{SFC}^{**}_{\mathrm{ME}}}{f_i\, \mathrm{DWT}\, f_w\, V_{\mathrm{ref}}}$$

Here, $P_{\mathrm{ME}(i)}$ and P_{AE} denote the power of the main and auxiliary engines, respectively. In addition, $P_{\mathrm{PTI}(i)}$, $P_{\mathrm{eff}(i)}$, and $P_{AE_{\mathrm{eff}(i)}}$ represent the contributions from shaft motors and innovative energy-efficient technologies. The coefficients C_{FME} and C_{FAE} correspond to fuel carbon factors, while SFC denotes the certified specific fuel consumption. Furthermore, the factors f_i, f_j, $f_{\mathrm{eff}(i)}$, and f_w account for capacity correction, power correction, the influence of innovative technologies, and speed reduction effects, respectively.

2.2 Correction Factors

The literature proposes various methods to estimate capacity and power correction factors for ice-class vessels, each based on different assumptions regarding ship performance and operating conditions.

2.2.1 Capacity Factor [f_i]

To account for reductions in ship capacity associated with ice-class reinforcement, capacity correction factors have been introduced in the literature and are commonly expressed as f_i [14], and defined in Eq. 4.

$$f_i = f_{i(\text{ice class})} \cdot f_{i_{C_b}} \tag{4}$$

The factors $f_{i(\text{ice class})}$ and $f_{i_{C_b}}$ represent the effects of hull ice strengthening and hull-form characteristics associated with ice-going performance. The factor $f_{i_{C_b}}$ is applicable to slow-speed ship types such as tankers, bulk carriers, and general cargo vessels. Ice-class ships typically exhibit lower block coefficients due to their more slender bow forms, which reduce cargo-carrying capacity compared to equivalent open-water designs [15]. Therefore, its value is constrained to be not less than 1.0, as shown in Eq. 5, and the average block coefficients for bulk carriers and tankers are given in Table 2.

$$f_{i_{C_b}} = \frac{C_{b\ \text{Reference Design}}}{C_{b\ \text{Ice-Class Design}}} \geq 1 \tag{5}$$

Table 2: Average block coefficients for bulk carriers and tankers for five size categories

Ship type	**Small**	**Handysize**	**Handymax**	**Panamax**	**Aframax**
	<10,000 DWT	10000 25000 DWT	25000 55000 DWT	55000 75000 DWT	75000 120000 DWT
Bulk carrier	0.78	0.80	0.82	0.80	0.83
Tanker	0.78	0.78	0.86	0.86	0.83

The factor $f_{i(\text{ice class})}$ is derived through regression analyses tailored to reflect the impact of different ice-class requirements [14] and is presented in Table 3. This factor is therefore directly related to changes in both lightweight and deadweight. Consequently, the reduced cargo-carrying capacity of ice-class vessels, compared to open-water ships of similar dimensions, leads to a reduction in deadweight. This effect is illustrated in Fig. 1, which compares deadweight for ships of equal length, as presented by Mazanikov [18].

Table 3: Capacity correction factor, f_i, representing additional steel used for ice hull strengthening across different ice classes, in relation to deadweight [14].

Ice Class	**Capacity Correction Factor** $f_{i(\textbf{ice class})}$
IC	$f_{i_{(\text{IC})}} = 1.0041 + \dfrac{58.5}{\text{DWT}}$
IB	$f_{i_{(\text{IB})}} = 1.0067 + \dfrac{62.7}{\text{DWT}}$
IA	$f_{i_{(\text{IA})}} = 1.0099 + \dfrac{95.1}{\text{DWT}}$
IAS	$f_{i_{(\text{IAS})}} = 1.0151 + \dfrac{228.7}{\text{DWT}}$

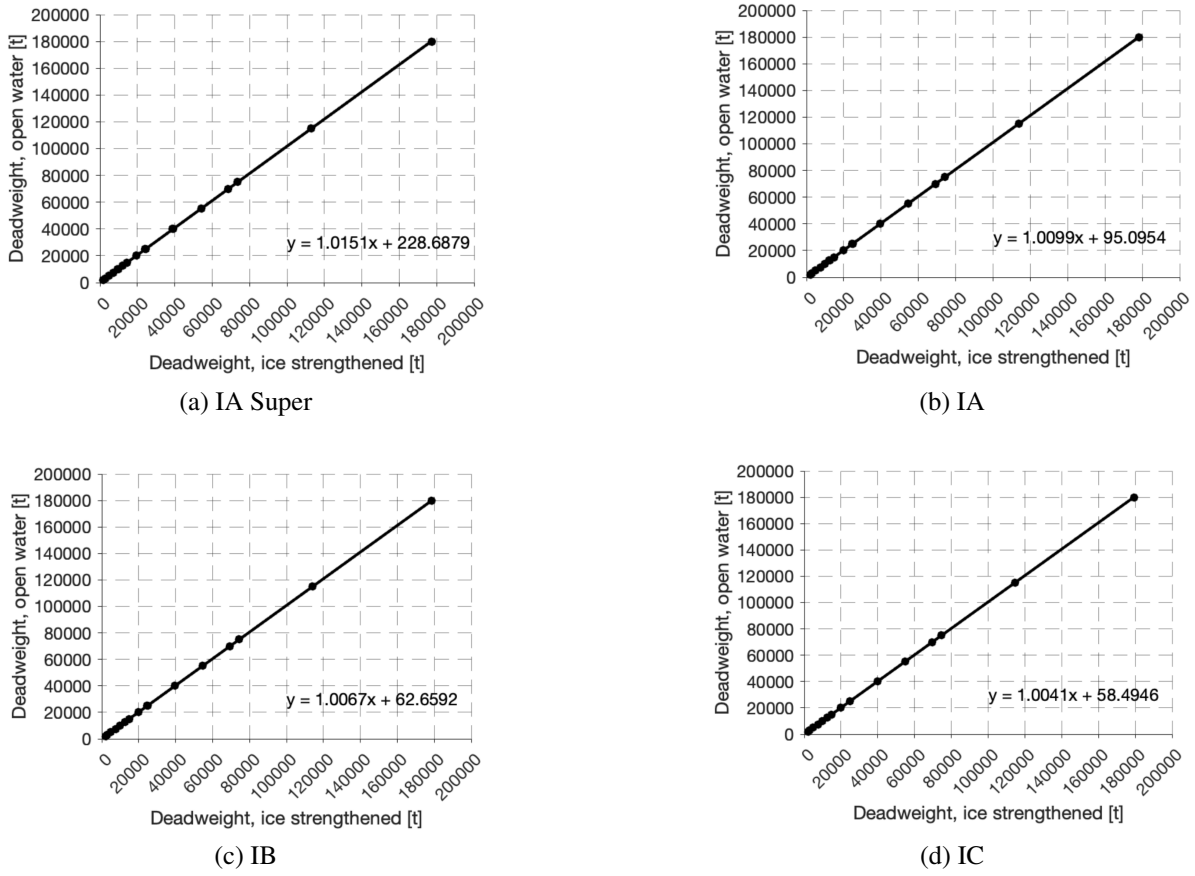

(a) IA Super

(b) IA

(c) IB

(d) IC

Figure 1: Decrease in deadweight due to ice strengthening of hull for different ice-class ships (adapted from [14], [18]).

To quantify the reduction in capacity due to ice-class reinforcement, the ship-specific voluntary structural enhancement correction factor, f_{iVSE}, is introduced. This factor represents the structural modifications required for an ice-class vessel to achieve performance comparable to an open-water ship. It is defined as the ratio of the deadweight of an open-water vessel to that of an ice-class vessel with the same displacement and steel grade, as shown in Eq. 6.

$$f_{iVSE} = \frac{DWT_{\text{Open Water}}}{DWT_{\text{Ice-Class Design}}} = \frac{\Delta - LWT_{\text{Open Water}}}{\Delta - LWT_{\text{Ice-Class Design}}} \tag{6}$$

Where Δ is the ship Displacement, $LWT_{OpenWater}$, $LWT_{Ice-ClassDesign}$ is the ships lightweight in open water and ice class conditions, respectively. Building on this research [14], which suggests that ice-class reinforcement leads to an approximately linear reduction in deadweight, Mazanikov [18] employed the rule-based Eq. 6 together with data from [14] to demonstrate the loss in deadweight resulting from a proportional increase in lightweight required to maintain constant displacement, as illustrated in Fig. 2. However, this represents an idealized scenario, and in practice, the increase in lightweight may exceed or fall below the corresponding reduction in capacity.

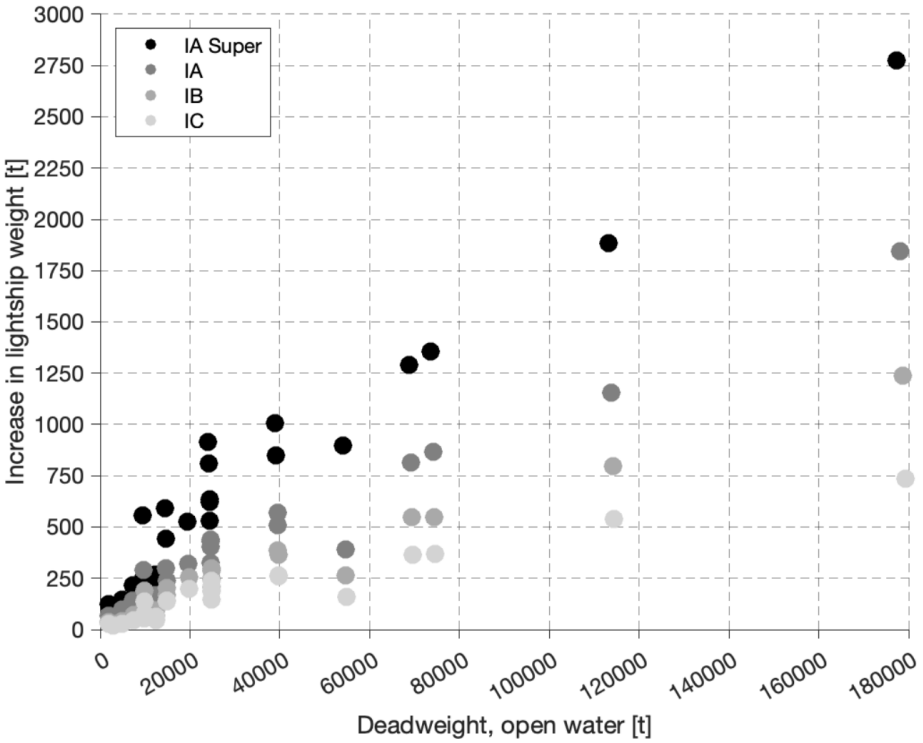

Figure 2: Weight increase for lightships as a result of ice strengthening for every kind of ship, taken from [18].

2.2.2 Power Correction Factor (f_j)

The significant power requirement for ice navigation requires the application of correction factors tailored to different ship types. These correction factors are calibrated based on average engine power. In more recent approaches, this power has been shown to correlate more consistently with deadweight tonnage (DWT) rather than the length between perpendiculars (L_{PP}), which was commonly used in earlier methods based on open-water ship designs [14].

The power correction factor f_j is defined by two limiting cases: the preliminary factor f_{j0} and the minimum required factor $f_{j,\min}$. The basic form is given by f_{j0}, defined as the ratio of the average open-water power to the actual installed power of the ice-class ship. This represents the upper limit of the correction, as shown in Eq. 7. However, the final value of f_j is governed by both f_{j0} and $f_{j,\min}$, the latter setting a lower bound. This ensures compliance with the minimum engine power requirements for the assigned ice class under the Finnish-Swedish Ice Class Rules, as given in Eq. 8.

$$f_{j0} = \frac{P_{aver,\ \text{ow(DWT)}}}{P_{\text{installed}}} \tag{7}$$

$$f_{j,min} = \frac{P_{aver,\ \text{ow(DWT)}}}{P_{aver,\ \text{ice(DWT)}}} \tag{8}$$

Where $P_{\text{aver, ow(DWT)}}$ and $P_{\text{aver, ice(DWT)}}$ denote the average engine power for non-ice-class (open-water) and ice-class ships, respectively, expressed as functions of the ship's deadweight. The term $P_{\text{installed}}$ refers to the actual installed propulsion power. For higher ice classes, significant differences in required engine power are observed, as these are typically determined through model testing rather than regression-based methods. In contrast, for lower ice classes, regression relationships derived from open-water ship data are generally considered sufficient. To address these discrepancies, EEDI guidelines were extended to include power correction factors for specific ship types such as reefers, in addition to conventional approaches based on ratios between open-water and ice-class propulsion power. These updated correction factors were introduced in Resolution MEPC.308(73) and are summarized in Table 4.

Table 4: Illustration of empirical equations for f_{j0} and $f_{j,\min}$ for different ship types [16].

Ship type	f_{j0}	$f_{j,\min}$			
		IAS	**IA**	**IB**	**IC**
Bulk carrier	$\frac{17.207 \cdot \text{DWT}^{0.5705}}{\sum_{i=1}^{n^{ME}} \text{MCR}_{ME_{(i)}}}$	$0.2515 \cdot \text{DWT}^{0.0851}$	$0.3918 \cdot \text{DWT}^{0.0556}$	$0.8075 \cdot \text{DWT}^{0.0071}$	$0.8573 \cdot \text{DWT}^{0.0087}$
Tanker	$\frac{17.444 \cdot \text{DWT}^{0.5766}}{\sum_{i=1}^{n^{ME}} \text{MCR}_{ME_{(i)}}}$	$0.2488 \cdot \text{DWT}^{0.0903}$	$0.4541 \cdot \text{DWT}^{0.0524}$	$0.7783 \cdot \text{DWT}^{0.0145}$	$0.8741 \cdot \text{DWT}^{0.0079}$
Cargo ship	$\frac{1.974 \cdot \text{DWT}^{0.7987}}{\sum_{i=1}^{n^{ME}} \text{MCR}_{ME_{(i)}}}$	$0.1381 \cdot \text{DWT}^{0.1435}$	$0.1574 \cdot \text{DWT}^{0.1440}$	$0.3256 \cdot \text{DWT}^{0.0922}$	$0.4966 \cdot \text{DWT}^{0.0583}$

2.3 Developed Method

The methodology adopted in this study for evaluating the capacity correction factor is based on estimating the increase in ship lightweight due to ice-class reinforcement. To assess its impact on the Attained EEDI, two approaches are considered: fixed displacement and fixed deadweight. These approaches are used to determine the resulting dimensional changes, which are subsequently applied to update the propulsion characteristics and recompute the Attained EEDI, as illustrated in Fig. 3.

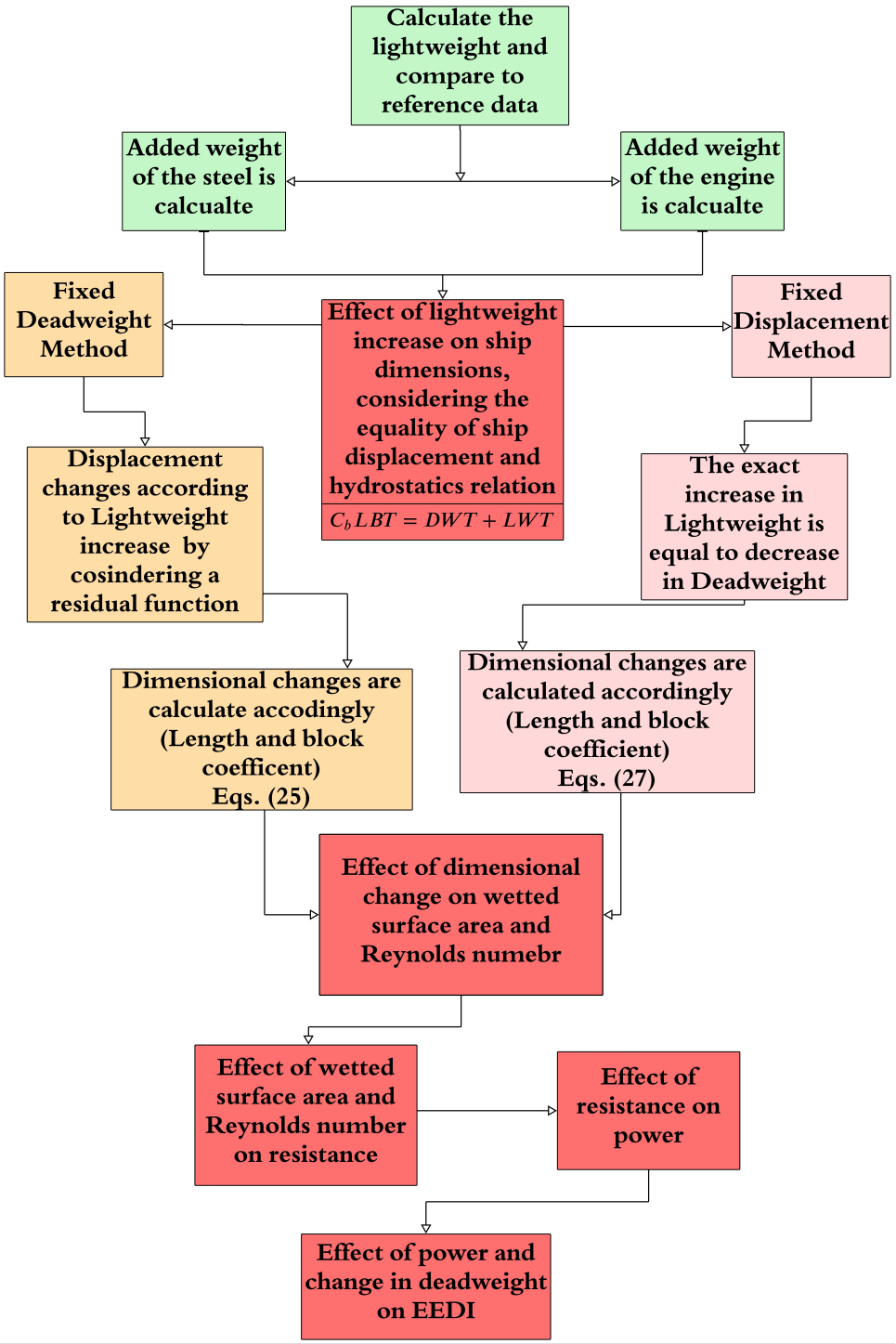

Figure 3: Flowchart of the two calculation methods used to account for the lightweight increase of ice-going ships, showing the resulting dimensional changes, updated power characteristics, and recalculated Attained EEDI.

According to Fig. 3, the methodology aims to quantify the impact of increased lightweight, due to ice-class reinforcement, on the ship's performance and Attained EEDI. The lightweight is first estimated using analytical approaches and validated against available reference data to ensure consistency. To evaluate its effect, two alternative approaches are adopted: the fixed deadweight method and the fixed displacement method. In the fixed deadweight approach, the displacement increases with added lightweight, whereas in the fixed displacement approach, the

deadweight is reduced accordingly. In both cases, the resulting changes in principal dimensions are used to update the hydrodynamic characteristics of the vessel, including resistance and required propulsion power, which are subsequently used to recompute the Attained EEDI.

2.3.1 Estimation of Lightweight

The total weight of a ship, referred to as its displacement (Δ), comprises two main components: deadweight (DWT) and lightweight (LWT). The lightweight is further divided into three primary components: steel structure weight (W_{St}), outfitting weight (W_O), and machinery weight (W_M), as expressed in Eq. 9.

$$\Delta = DWT + LWT = DWT + [W_{St} + W_O + W_M] \tag{9}$$

The contribution of these components to the total lightweight varies depending on the vessel type, as illustrated in Table 5. Among them, the steel structure weight generally constitutes the largest share and therefore has the greatest influence on variations in lightweight. This is particularly relevant for ice-going ships, where additional steel is required for hull strengthening. It is therefore essential to assess the impact of increased steel weight when analyzing design adaptations for higher ice-class vessels.

Table 5: Percentage of various weight groups relative to light ship weight [21].

	Ship type and size	DWT/Δ [%]	W_{St}/Δ_L [%]	W_O/Δ_L [%]	W_M/Δ_L [%]
Cargo ship	5000–15 000 tdw	60–80	55–64	19–33	11–22
	Coastal cargo ship 499–999 GT	70–75	57–62	30–33	9–12
Bulker	20 000–50 000 tdw	74–80	68–79	10–17	12–16
	50 000–150 000 tdw	80–87	78–85	6–13	8–14
Tanker	25 000–120 000 tdw	65–83	73–83	5–12	11–16
	$\geq$200 000 tdw	83–88	75–83	9–13	9–16
Containership	10 000–15 000 tdw	60–76	58–71	15–20	9–22
	20 000–50 000 tdw	60–70	62–72	14–20	15–18

The present methodology focuses on bulk carriers, for which empirical relationships for lightweight estimation are well established in the literature. The analysis aims to evaluate how increase in ice-strengthening requirements influence lightweight, and consequently displacement and propulsion power. Although in principle, changes in main dimensions such as ship length may compensate for reduced cargo capacity, empirical length–weight relationships derived from open-water vessels are not directly applicable to ice-class ships. This limitation necessitates a more careful treatment of lightweight estimation. As summarized in Table 5, the lightweight is composed of distinct components that must be evaluated separately. These components are estimated using established empirical formulations presented by Schneekluth [21].

1. Outfitting Weight:

   The outfitting weight (W_O) includes shipboard systems and auxiliary components such as electrical installations, auxiliary machinery, and deck equipment. This category also accounts for non-structural elements required for vessel operation and accommodation, which in this study is estimated using the empirical formulation proposed by Watson and Gilfillan [31].

$$W_o = C_o \cdot L \cdot B \text{ (tons)} \tag{10}$$

Where B, L are breadth and length, and the outfit coefficient, C_o, is chosen based on the ship type and length as detailed in [24]. For bulk carriers, this coefficient varies between 0.19 and 0.25, depending on the specific length of the vessel.

2. Machinery Weight:

   The machinery weight can be estimated using engine power and speed, using the maximum continuous rating (MCR) and a coefficient C_m, which for bulk carriers is 0.72. The calculation method is detailed in [21].

$$W_m = C_m \cdot \text{MCR}^{0.78} \text{(tons)} \tag{11}$$

3. Structural Weight:

   The calculation of steel weight across different ship types is one of the most debated aspects of lightweight estimation, as various methods and researchers present differing approaches.

   (a) Murray [26] :

$$W_s^{\text{Murray}} = \frac{0.026 \cdot L^{1.65} \cdot (B + D + \frac{T}{2}) \cdot (0.5 \cdot C_b + 0.4)}{0.8} \text{(tons)} \tag{12}$$

   (b) DNV [28]:

$$W_s^{\text{DNV}} = 4.274 \cdot W^{0.62} \cdot L \cdot \left(1.215 - 0.035 \cdot \frac{L}{B}\right) \cdot \left(0.73 + 0.025 \cdot \frac{L}{B}\right) \cdot \left(1 + \frac{L - 200}{1800}\right) \cdot \left(2.42 - 0.07 \cdot \frac{L}{D}\right) \cdot \left(1.146 - 0.0163 \cdot \frac{L}{D}\right) \text{(tons)} \tag{13}$$

   Where W is the section modulus of the midship area.

   (c) Watson and Gilfillan [31]:

$$E = L(B + T) + 0.85L(D - T) + 0.85L_s H_s \tag{14}$$

$$W_s^{\text{Gilfillan}} = K \cdot E^{1.36} \cdot (1 + 0.5(C_b - 0.7)) \text{ (tons)} \tag{15}$$

   Where L_s and H_s are the length and height of the superstructure and E is a weight coefficient based on the dimensions as shown in Eq. 14.

   (d) Harvald and Jensen [32]:

$$C_s = 0.07 + 0.064 \cdot \exp\left(-\left(0.5u + 0.1u^{2.45}\right)\right) \tag{16}$$

   u is a weight coefficient based on the dimensions mentioned in [32].

$$W_s^{\text{Harvald}} = L \cdot B \cdot D \cdot C_s \text{(tons)} \tag{17}$$

To assess the effect of increased lightweight on hull length, the lightweight estimation methods are first validated. For this purpose, a set of bulk carriers listed in Table 15 is selected. The

lightweight of each vessel is estimated using the selected methods and subsequently compared with the corresponding actual values. The relative error is presented in Fig. 4. Among the evaluated methods, the approach proposed by Watson and Gilfillan [31] provides the most accurate estimates, with an average error of 12% and a standard deviation of 16% across the range of ship sizes considered.

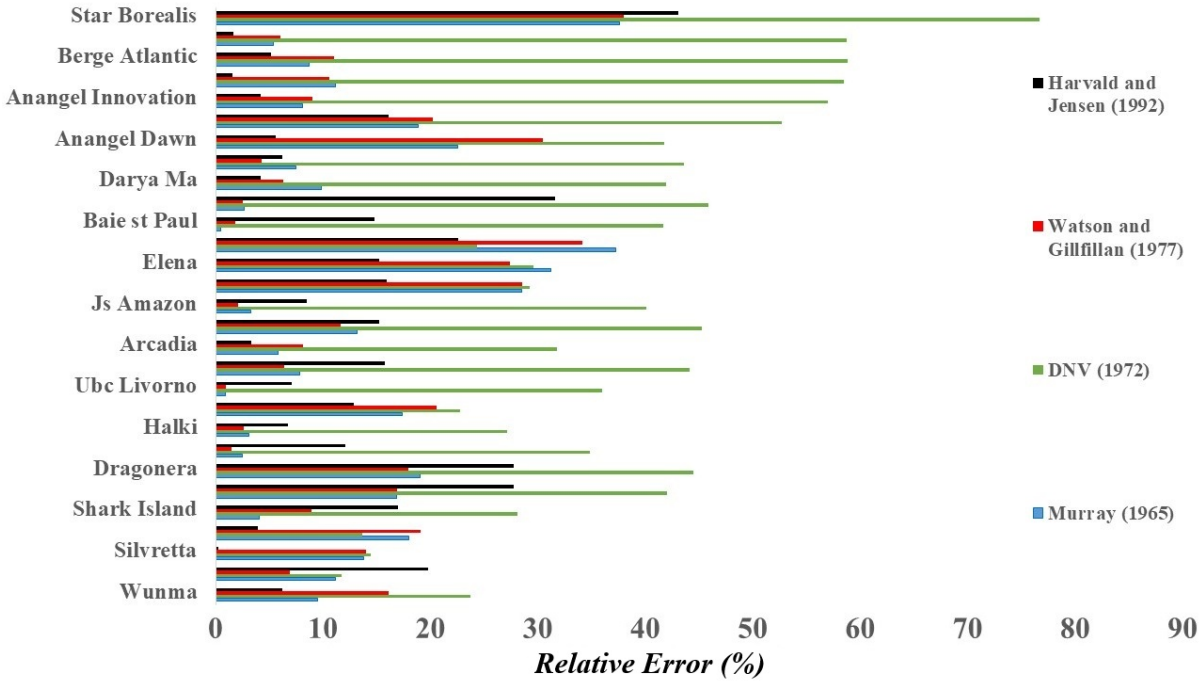

Figure 4: Estimation of Lightweight based on different methods.

2.3.2 Estimation of Added Weight

As mentioned, ice-going ships typically have a higher lightweight due to additional steel reinforcement and heavier machinery. This increase must be properly accounted for in the analysis. The added lightweight is expressed as a fraction of the original lightweight, denoted by α. Since the increase arises from two distinct sources, it is decomposed into α_1 for the additional steel and α_2 for the increased machinery weight.

- **Added Steel Weight**

Steel weight increase is expressed as the ratio of added steel, including voluntary structural enhancement as shown in Eq. 6, to the original lightweight, while the corresponding deadweight increase is derived from the capacity correction factor in Fig. 1.

$$\alpha_1 = \frac{LWT_{ice}}{LWT_{ow}} = \frac{(\Delta_{ow} - [\frac{DWT_{ice}}{DWT_{ow}} \times (\Delta_{ow} - LWT_{ow})])}{LWT_{ow}} \tag{18}$$

where DWT_{ow}/DWT_{ice} is presented in Fig.1. Also, according to [14], analysis of numerous ships comparing open-water and ice-going vessels of similar size and deadweight indicates these values are approximately 106.40% for IA Super, 105.23% for IA, 103.53% for IB, and 102.36% for IC.

- **Added Engine Weight**

According to the guidelines detailed in Sec. 2.2.2, the power correction factor is determined based on the vessel's deadweight. The procedure for calculating this factor is systematically presented in Table 4. Consequently, Fig. 5 demonstrates that with a higher ice class, the required power correction factor significantly increases. Also, the minimum power correction factor needed for achieving ice class IC status surpasses the standard requirements.

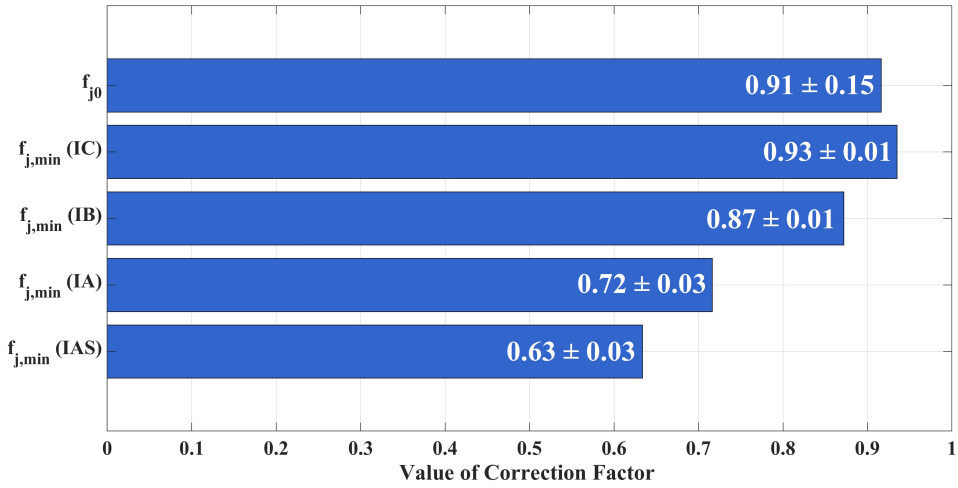

Figure 5: Illustration of attained power correction factor for all ships mentioned in Table 15 using information in Table 4.

In addition to the increase in steel weight, the contribution of machinery weight must also be considered. As indicated in Table 15, machinery weight typically accounts for approximately 7.87% ± 1.77% of the total lightweight. This proportion varies with vessel size, being around 5% for larger ships and increasing to approximately 13% for smaller vessels. The increase in machinery weight is primarily driven by the higher propulsion power required for ice-going operation. As illustrated in Fig. 5, ice-class ships require larger and more powerful engines compared to their open-water counterparts.

α_2 is the sole rise from changes in machinery, without accounting for structural reinforcement effects. The corresponding increase in lightweight due to machinery modifications is defined in Eq. 19. Based on this assumption, the resulting variation in lightweight for different ice classes is presented in Table 6.

$$\alpha_2 = \frac{LWT_{ow} + C_m((\frac{f_{j0}}{f_{j,min}} \times MCR_{ow})^{0.78} - MCR_{ow}^{0.78})}{LWT_{ow}} \tag{19}$$

Table 6: Impact of engine modifications on MCR and LWT across different ice classes for ships presented in Table 15.

Ice class	MCR (MW)	LWT (kt)	Increase in MCR (%)	Increase in LWT (%)
OW	10.05 ± 4.26	12.98 ± 66.51	-	-
IC	9.64 ± 2.87	12.95 ± 6.49	-2.01 ± 15.85	-0.22 ± 1.04
IB	10.35 ± 4.16	13.01 ± 6.51	5.06 ± 17.01	0.20 ± 1.05
IA	12.43 ± 4.82	13.16 ± 6.52	27.91 ± 20.92	1.59 ± 1.14
IAS	13.96 ± 4.56	13.26 ± 6.53	44.75 ± 23.07	2.58 ± 1.31

Table 6 shows that equipping open-water ships with ice-class engines for classes IAS, IA, and IB leads to an increase in both MCR and lightweight. In contrast, for class IC, the machinery modification results in a slight reduction in lightweight, indicating a comparatively lower propulsion requirement.

The influence of both is summarized in Eq. 20, where the combined steel and engine changes yield weight ratios (α): 108.98% for IA Super, 106.82% for IA, 103.78% for IB, and 100.16% for IC.

$$\alpha = \alpha_1 + \alpha_2 \tag{20}$$

2.3.3 Impact of Lightweight Increase on Ship Dimensions Under Fixed Deadweight

This section estimates the required increase in ship length to compensate for lightweight growth under a fixed deadweight constraint. When deadweight is fixed, an increase in lightweight leads directly to an increase in displacement. This requires adjustments in key design parameters such as length, breadth, draft, or block coefficient. However, increasing breadth would significantly raise ice resistance in channels, while increasing draft may limit port accessibility. Therefore, designers typically keep breadth and draft constant, making hull lengthening the most feasible solution. This approach results in a more slender hull form, which is used in the following analysis to estimate the corresponding increase in vessel length.

- **Estimation of Increase in Length**

Lightweight was calculated using Eqs. 10, 11, and 15 and shown as $LWT(L)$ in Eq. 21, while deadweight was held constant through Eq. 9. Based on these assumptions, the corresponding enlargement of the ship was then estimated. The ship length L is determined such that the hydrostatic displacement equals the sum of deadweight and lightweight:

$$C_b LBT = \mathrm{DWT} + \mathrm{LWT}(L) \tag{21}$$

Defining the residual function:

$$\mathrm{RES}(L) = C_b LBT - (\mathrm{DWT} + \mathrm{LWT}(L) + W_I) \tag{22}$$

Where W_I is the effect of ice strengthening on lightweight is expressed as a proportional increase relative to the open-water design:

$$\mathrm{W_I} = \alpha \ \times \mathrm{LWT_{open}} \tag{23}$$

The solution requires $\mathrm{RES}(L) = 0$, where the lightweight function is modeled based on Newton iteration:

$$\frac{d\,\mathrm{RES}}{dL} = C_b BT - \frac{d(\,\mathrm{LWT}(L))}{dL} \tag{24}$$

The iteration proceeds as

$$L_{n+1} = L_n - \frac{\mathrm{RES}(L_n)}{\frac{d\,\mathrm{RES}}{dL}(L_n)}, \tag{25}$$

starting from $L_0 = L_{\mathrm{ow}}$. Convergence is achieved when

$$|\mathrm{RES}(L_{n+1})| < \varepsilon \text{ which is approximately } (10^{-10}) \tag{26}$$

2.3.4 Impact of Lightweight Increase on Ship Dimensions Under Fixed Displacement

The alternative approach evaluates changes within a fixed displacement framework, where any increase in lightweight is offset by a corresponding reduction in deadweight. This scenario is particularly relevant when modifying the main dimensions to reduce the block coefficient, thereby improving bow performance for ice-breaking operations. To account for the increase in hull length, the increase in lightweight due to ice strengthening (LWT_{ice}) is calculated according to Eq. 27. While the constant-displacement assumption is applied, Eq. 22 remains valid to describe the overall dimensional constraints. With a known increase in lightweight, the modified length (L_{ice}) and corresponding block coefficient ($C_{b_{ice}}$) are the only unknowns. These parameters are determined using the lightweight estimation equations, namely Eqs. 10, 11, and 15, as summarized in Eq. 27.

$$\begin{aligned} LWT_{ice} = K\Big[\, L_{ice}(B+T) + 0.85\, L_{ice}(D-T) + 0.85\, L_s H_s \,\Big]^{1.36} \Big(1 + 0.5\big(C_{b_{ice}} - 0.7\big)\Big) \\ + C_m\,(\mathrm{MCR})^{0.78} + C_o\, L_{ice} B, \\ \text{where } C_{b_{ice}} = \frac{L_{PP_{OW}}}{L_{PP_{ice}}} \times\ C_{b_{OW}} \end{aligned} \tag{27}$$

There is no closed-form algebraic solution because ice-going ship length L_{ice} appears both inside a non-integer power term and as a reciprocal term within the same expression. This combination makes the equation transcendental, meaning it cannot be simplified or solved using algebraic manipulation. Therefore, numerical root-finding methods, such as the Newton-Raphson, must be used to find an approximate solution for ice-going ship length L_{ice}.

2.3.5 Estimation of Propulsive Power

Following the estimation of hull length and displacement changes, propulsive power can be evaluated based on the total resistance encountered at a given speed. This resistance comprises frictional, residual, and air resistance components. The governing equations, which allow esti-

mation of propulsive power for different operating conditions, are as follows.

$$P_E = R_T \times V \tag{28}$$

$$R_T = R_F + R_R + R_A \tag{29}$$

In this study, conducted at a constant velocity, changes in power are directly related to changes in resistance. Identifying the dominant factor in ship resistance requires examining flow behavior. Larsson [23] demonstrated that frictional resistance is the most significant component for slow-moving bulk carriers, as shown in Fig. 6.

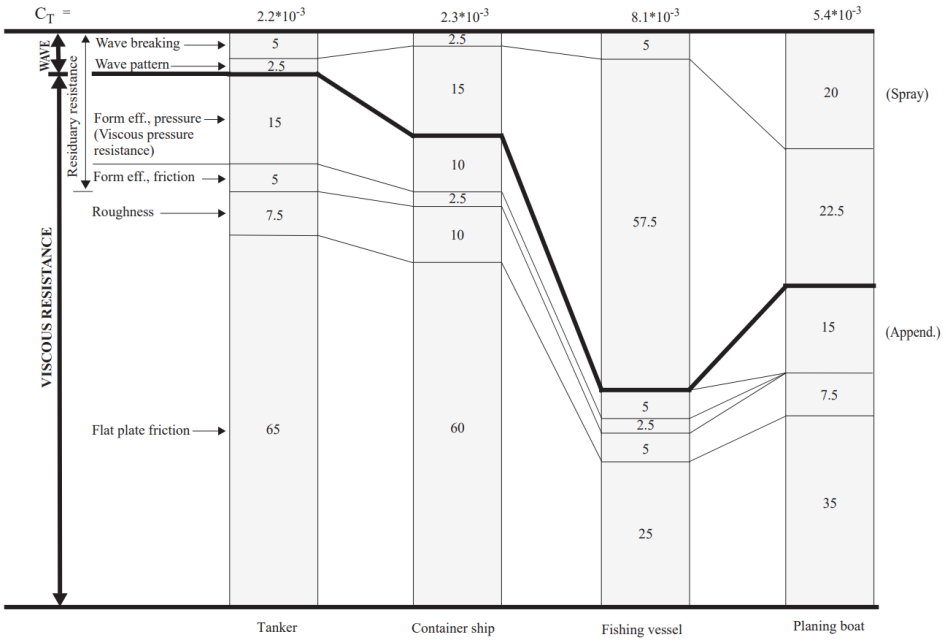

Figure 6: Resistance components for four vessels (%) Larsson [23].

Consequently, frictional resistance is the most influential component. Calculating a ship's total resistance is a complex process that typically requires model testing or advanced Computational Fluid Dynamics (CFD) simulations. However, for simplified analysis, several empirical equations can provide reasonable estimations of the resistance. In such cases, it is often assumed that total resistance is approximately equal to frictional resistance, while variations in residual and air resistance are minor and negligible. Therefore, the total resistance can be equated to the frictional resistance, as expressed in Eq. 30.

$$R_T \approx R_F = \frac{1}{2} C_F \rho S V^2 \tag{30}$$

The factors in Eq. 30 include C_F , the frictional coefficient, which is determined using the ITTC guidelines [25] as shown in Eq. 31. The wetted surface area S must be reported or estimated; for bulk carriers, an approximation based on Lap [38] is given in Eq. 33.

$$C_F = \frac{0.075}{(log_{10} Re - 2)^2} \tag{31}$$

$$Re = \frac{\rho U L}{\mu} \tag{32}$$

$$S = \Delta^{(\frac{1}{3})} \cdot (3.4 \cdot \Delta^{(\frac{1}{3})} + 0.5 . L_{LW}) \tag{33}$$

Where L_{LW} is the length of the water line. At a constant velocity of 10 knots, power is directly related to hydrodynamic resistance, which in this case is dominated by frictional resistance. Changes in power are therefore derived from the geometric modifications that alter wetted surface area, Reynolds number, and the friction coefficient, allowing an isolated assessment of the effects of geometry. To investigate this, data from a representative bulk carrier (Fig. 4) and reported lightweight increases for various ice classes are used. By applying the Newton–Raphson method to Eq. 25, the resulting length increase can be determined. This length change affects the Reynolds number (Eq. 32), altering the frictional coefficient (Eq. 31) and increasing the wetted surface area (Eq. 33). Together, these effects elevate the total resistance (Eq. 30), which directly raises the required power at a fixed operating speed.

2.3.6 Estimation of Increase in EEDI

According to the EEDI formulation in Eq. 3, the proportional change in the Attained EEDI can be calculated by considering both the reduction in deadweight and the corresponding increase in required power. This relationship is described in Eq. 34 yielding an alternative formulation for the EEDI calculation:

$$\text{Attained EEDI} = \frac{\text{Power} \times \text{SFC} \times C_F}{\text{DWT} \cdot V_{ref}} \tag{34}$$

Where SFC = specific fuel consumption (g/kWh), C_F = carbon emission factor (gCO_2/g fuel), and DWT can therefore be expressed as a function of the displacement and the lightweight, assuming all other parameters remain constant.

Fixed Displacement

In this scenario, an increase in lightweight directly corresponds to a reduction in deadweight, as ice strengthening adds to the vessel's weight while decreasing its cargo-carrying capacity. If the vessel undergoes dimensional changes, the power input would also change, subsequently affecting the Attained EEDI value.

To simplify calculations, we consider the ratio of change in deadweight, defined as the difference between displacement and lightweight, and the corresponding ratio $\frac{\Delta}{LWT}$, denoted as β. This is used alongside the lightweight increase factor α. Using these, we can estimate the variation in EEDI when transitioning from an open-water ship to an ice-class vessel.

$$\frac{EEDI_{Ice}}{EEDI_{OW}} = \frac{\frac{P_{IC}}{(\Delta_{OW} - \alpha LWT_{OW})}}{\frac{P_{OW}}{(\Delta_{OW} - LWT_{OW})}} = \frac{(\Delta_{OW} - \frac{\Delta_{OW}}{\beta})}{(\Delta_{OW} - \alpha\frac{\Delta_{OW}}{\beta})} \times \frac{P_{IC}}{P_{OW}} = \frac{\beta - 1}{\beta - \alpha} \times \frac{P_{IC}}{P_{OW}} \tag{35}$$

For the scenario described in Sec. 3.1.1, where there are no dimensional changes, the difference in power is zero, and Eq. 36 can be rewritten as:

$$\frac{EEDI_{Ice}}{EEDI_{OW}} = \frac{\beta - 1}{\beta - \alpha} \tag{36}$$

Fixed Deadweight

In scenarios with fixed deadweight, changes in the denominator are fixed, but variations in the lightweight significantly impact the required power, primarily altering resistance. According to the IMO document [27], propulsion power is assumed to account for approximately 85% of a ship's total power, so any increase in this area directly affects the Attained EEDI, which can be expressed as:

$$\frac{EEDI_{Ice}}{EEDI_{OW}} = 0.85 \times \frac{P_{IC}}{P_{OW}} \tag{37}$$

3 Result

Two methodologies are applied to quantify the effect of increased lightweight and capacity changes on the EEDI. In the first approach, a capacity correction factor is introduced to offset the increase in EEDI. In the second approach, the effect of additional steel weight and the resulting engine modifications is evaluated. Each parameter is varied individually to isolate its impact on the overall vessel design.

3.1 EEDI Changes: Capacity Correction with Extra Steel Weight

3.1.1 Fixed Displacement without Dimensional Changes

In the first scenario, displacement is kept constant, and any increase in lightweight results in a corresponding decrease in deadweight, without dimensional changes. Under these conditions, the EEDI depends solely on the deadweight term in the denominator. Consequently, the increase in EEDI is governed by two parameters: the displacement-to-lightweight ratio, β, and the ice-strengthening factor, α. The value of β is fixed based on the data in Table 15. α one the other hand, is determined from two separate sources. First, the additional steel weight defined in Eq. 18. Second, the literature estimates indicate that ice strengthening increases lightweight by approximately 10–12% for IA Super, 5–7% for IA, 3–4% for IB, and 1–2% for IC [22, 17, 13]. Therefore, the amount of increase in EEDI is calculated based on Eq. 36 and presented in Table 7.

Table 7: Estimated of increase EEDI considering different values for the ratio of increase in the lightweight (α).

Ice class	**IAS**	**IA**	**IB**	**IC**
ΔEEDI (%) ([22, 17, 13])	2.49 ± 0.45	1.40 ± 0.33	0.79 ± 0.22	0.34 ± 0.14
ΔEEDI (%) ([14])	1.53 ± 0.45	1.25 ± 0.33	0.85 ± 0.22	0.56 ± 0.14

Table 7 shows that higher values of α lead to a non-uniform increase in EEDI across different ice classes, with IA Super exhibiting a larger capacity correction factor than that specified in the regulations. Furthermore, the corresponding increase in steel weight is more consistent with the values reported by [14]. Therefore, these values are adopted in the subsequent analysis.

3.1.2 Fixed Displacement with Dimensional Changes

An alternative approach with fixed displacement allows the vessel dimensions to vary in response to increased lightweight due to ice-class requirements. To maintain constant displacement, the block coefficient decreases proportionally as the vessel length increases. The required increase in lightweight is determined by the selected ice class (Fig. 2). Based on this increase, the corresponding changes in vessel dimensions are calculated using Eq. 27. These geometric modifications affect both the wetted surface area and the required propulsion power, as described in Eqs. 33 and 28, respectively. The resulting changes are summarized in Table 8.

Table 8: Estimation of the impact of additional weight from ice strengthening on the dimensions and performance parameters of an equivalent open-water ship under fixed displacement constraints.

Ice Class	ΔL **(%)**	ΔC_b **(%)**	ΔS **(%)**	ΔP **(%)**
IAS	6.80 ± 0.53	-6.80 ± 0.53	3.10 ± 0.21	2.40 ± 0.16
IA	5.63 ± 0.52	-5.63 ± 0.52	2.53 ± 0.19	1.96 ± 0.15
IB	3.89 ± 0.37	-3.89 ± 0.37	1.71 ± 0.13	1.33 ± 0.10
IC	2.63 ± 0.21	-2.63 ± 0.21	1.15 ± 0.07	0.89 ± 0.05

As shown in Table 8, higher ice classes require a greater reduction in C_b and a corresponding increase in ship length. Although Eq. 33 indicates that ship length influences the wetted surface area, it is not the dominant parameter, as the wetted surface area increases only marginally despite the increase in length. However, this increase still leads to higher propulsion power requirements. In addition, the reduction in capacity, resulting from the lower block coefficient, affects the EEDI through its presence in the denominator, thereby increasing the attained EEDI (Eq. 34). The resulting change in EEDI, calculated using Eq. 35, is presented in Table 10.

3.1.3 Fixed Deadweight with Increase in Length

The fixed deadweight method described in Sec. 2.3.3 is used as an alternative calculation approach in this analysis. In contrast to the previous case, the change in length is independent of the block coefficient, and the dimensional adjustment is therefore limited to the ship length. The length variations for the different ships were calculated using Eq. 25. For the particular ice class of IAS, the increase in ship length obtained using the fixed deadweight method varies as shown in Fig. 7, where the increase is presented for a particular β.

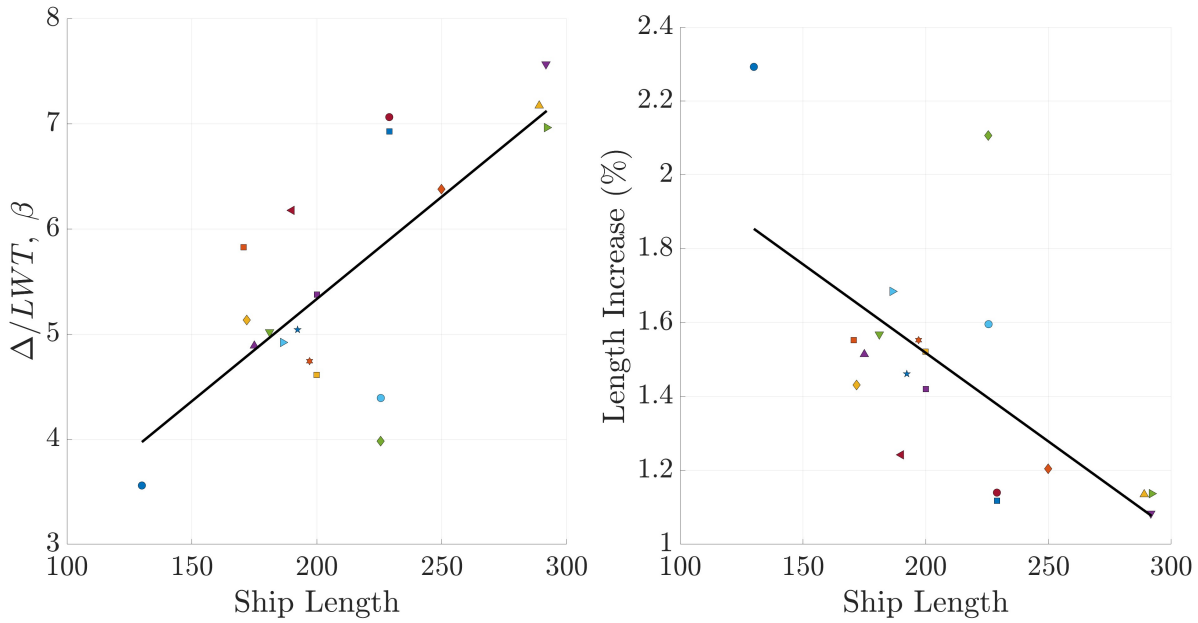

Figure 7: Displacement-to-lightweight ratio (β) and increasing ship length with respect to the length for various vessels.

As shown in Fig. 7, shorter and lighter ships experience the largest relative increase in length under ice strengthening, while longer and heavier ships elongate less. With larger ships, the displaced volume grows quicker with length than the lightweight. Thus, both ship length and displacement-to-lightweight ratio inversely correlate with the percentage increase in length. Also, the increase in ship length corresponds to the increase in displacement, as length is the only variable that changes in this analysis. Based on Table 9, there is a linear relationship between the increase in length and the increase in the power.

Table 9: Estimation of the impact of additional weight from ice strengthening on the dimensions and performance parameters of an equivalent open-water ship under fixed deadweight with constant C_b.

Ice Class	ΔL **(%)**	ΔS **(%)**	ΔP **(%)**
IA Super	1.46 ± 0.31	1.44 ± 0.32	1.30 ± 0.29
IA	1.19 ± 0.25	1.19 ± 0.26	1.06 ± 0.24
IB	0.80 ± 0.17	0.80 ± 0.17	0.71 ± 0.16
IC	0.53 ± 0.11	0.53 ± 0.12	0.48 ± 0.10

As shown in Table 9, an increase in lightweight for higher ice classes results in longer ships, necessitating greater power. However, Table 8 indicates a different scenario. When displacement is constant, changes in wetted surface area are minimal, reflecting only half the change in length. In contrast, when displacement increases with length, the wetted surface area expands significantly, nearly in a 1:1 ratio with the length change. This substantial increase in wetted surface area results in a greater power demand compared to cases where displacement is kept constant.

3.1.4 Fixed Deadweight with Increase in Length and Reduction in C_b

In the next step, length and block coefficient changes are considered together. However, in this approach, we specifically control and adjust the block coefficient, systematically reducing it by 1–4% to evaluate its impact on the solution. Eq. 15 was employed to estimate the lightweight based on ship length and block coefficient, while Eq. 22 was used to determine the corresponding increase in length for each reduction in C_b. Similarly to the previous calculations, the resulting variations in the length of the ship and the block coefficient were applied to evaluate their effects on displacement and power requirements, as illustrated in Fig. 8.

Although a lower C_b slightly decreases the friction coefficient due to a higher Reynolds number, the overall resistance and required power increase notably. The wetted surface area dominates the moderate C_F reduction. Consequently, the Attained EEDI rises proportionally with power, reflecting geometric and hydrodynamic effects of reduced C_b. Fig. 8 shows that in the IAS class, length rises from 2.8 to 6.3 (over 100% increase), while lower ice classes show smaller but consistent growth. This indicates that more heavily strengthened vessels require greater geometric adjustment to compensate for the added lightweight.

According to Table 8, for the ice class IAS, increasing the ship length by 6.8% leads to that exact amount of reduction in the block coefficient, and the wetted surface area increases by only 3.10%. In contrast, when the deadweight is kept constant, for the case of IAS in the systematic reduction of block coefficient to 4%, the increase in wetted surface area is 4.2%. This increase explains why the power requirements of the scenario under fixed deadweight conditions (Fig. 8) are higher than those under fixed displacement conditions, as reported in Table 9.

3.1.5 Comparison of Attained EEDI

The calculated EEDI values obtained from the different methodologies are compared in Table 10. The change in EEDI described in Sec. 2.3.6 was quantified using the calculation methods presented in Secs. 3.1.1, 3.1.2, 3.1.3 and 3.1.4. The results are shown together with the rule-based correction factors given in Table 3, allowing the different scenarios to be evaluated on a consistent basis.

Table 10: Comparison of estimated EEDI under the effect of extra steel weight using fixed displacement, fixed deadweight, and the capacity correction factor mentioned by the regulations.

Ice Class	**IAS**	**IA**	**IB**	**IC**
Capacity Correction Factor (%)	2.07 ± 0.42	1.14 ± 0.17	0.82 ± 0.11	0.50 ± 0.10
EEDI ↑ (%) (Fixed DWT with L↑)	1.11 ± 0.29	0.91 ± 0.24	0.60 ± 0.16	0.41 ± 0.11
EEDI ↑ (%) (Fixed Δ)	1.53 ± 0.45	1.25 ± 0.33	0.85 ± 0.22	0.56 ± 0.14
EEDI ↑ (%) Fixed DWT with L↑, $C_b(4\%)$ ↓	2.94 ± 0.51	2.73 ± 0.45	2.42 ± 0.37	2.21 ± 0.31
EEDI ↑ (%) (Fixed Δ with L↑, C_b ↓)	3.95 ± 0.41	3.22 ± 0.26	2.17 ±0.17	1.49 ± 0.14

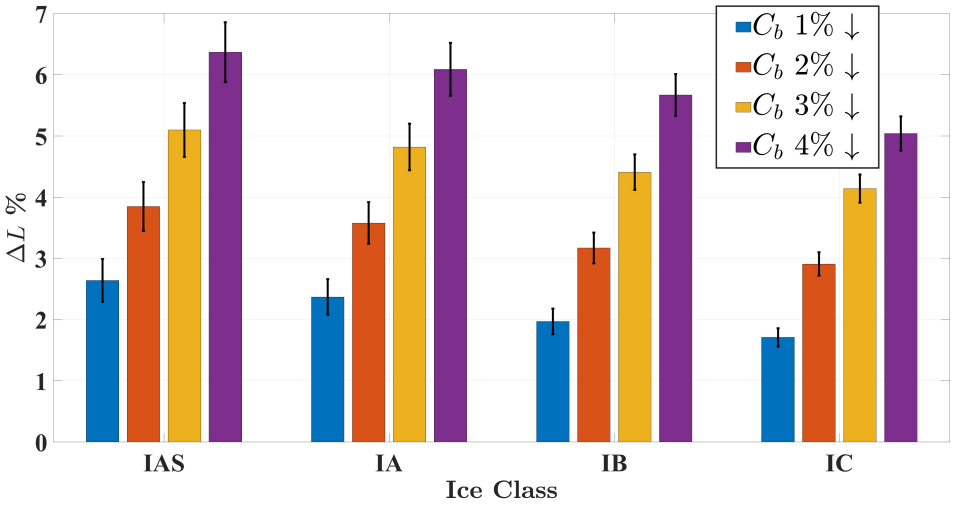

(a) Increase in Length

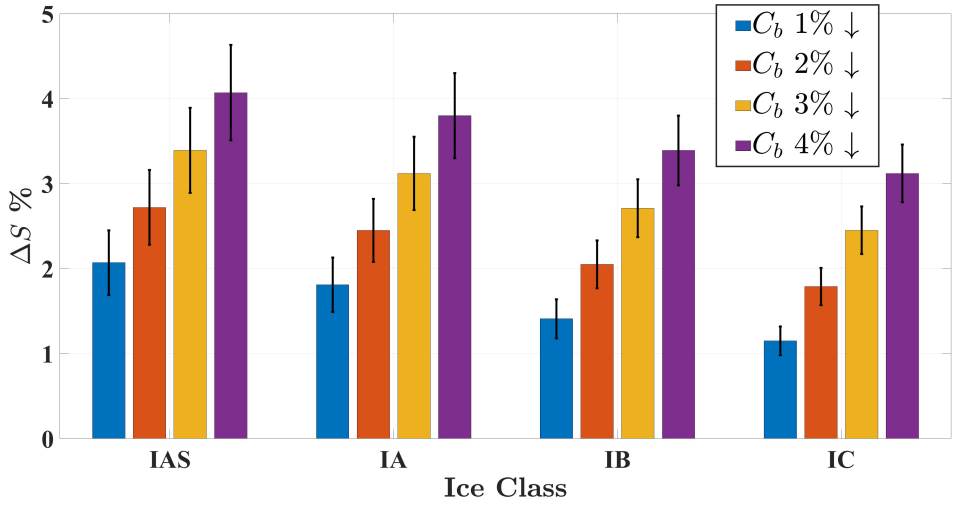

(b) Increase in Wetted Surface Area

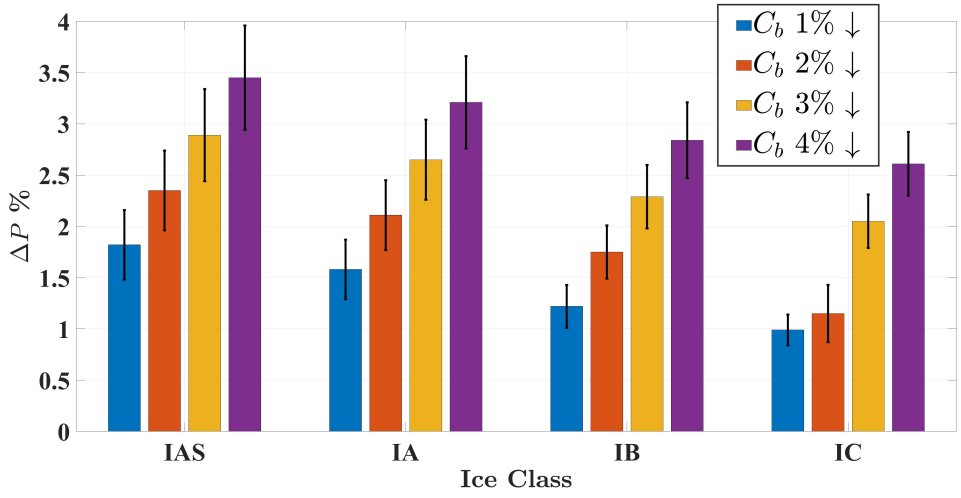

(c) Increase in Power

Figure 8: Estimation of the impact of additional weight from ice strengthening on the dimensions and performance parameters of an equivalent open-water ship under fixed deadweight with various C_b.

As depicted in Table 10, to obtain an average number for correction factors reported in the regulations, the equations mentioned in (Table 3) are derived by using the reference data ships (Table 15). In an ideal scenario with no dimensional changes, values are consistent for lower ice classes. However, for an equivalent ship where modifications are based on fixed deadweight with dimensional changes, the decreased capacity effect is underestimated.

In the fixed displacement scenario with dimensional changes, the equivalent ship requires a further capacity correction factor. Likewise, an equivalent ship with fixed deadweight experiences more substantial changes relative to the base capacity correction factor. When comparing these scenarios, the primary alteration in the fixed displacement case stems from changes in deadweight, a key factor in EEDI calculations, as it remains fixed in the denominator for the other case. Moreover, the increase in power is more pronounced in the fixed deadweight scenario, as demonstrated in Fig. 8, compared to the fixed displacement case shown in Table 8, due to the significant increase in wetted surface area. Although power is a critical factor, a change in deadweight can increase the amount of EEDI as well, and that explains the more pronounced increase when the deadweight and power change at the same time in the fixed displacement case.

3.2 EEDI Changes: Capacity Correction with Extra Steel and Machinery Weight

In the previous section, the effect of the additional ice-strengthening weight on the equivalent open-water ship was evaluated. In addition to the increase in structural steel weight, the transformation to the ice-class configuration also requires modifications to the propulsion machinery, including the installation of a new engine. Therefore, this section examines the combined effect of the increased steel weight and the modified machinery weight on the ship characteristics.

3.2.1 Fixed Displacement without Dimensional Changes

The impact of machinery weight was evaluated based on the increase in Maximum Continuous Rating (MCR), as detailed in Table 6. This assessment included the effect of additional steel on lightweight, as described by Eq. 20 to have both the effect of engine modification and extra steel. For this scenario, the new weight ratios are 108.98% for IA Super, 106.82% for IA, 103.78% for IB, and 100.16% for IC. Notably, IA Super and IA exhibit increases compared to previous factors, while IB remains relatively unchanged and IC experiences a reduction. This reduction is attributed to the ships in Table 15 possessing sufficient power for IC, allowing for smaller engines to offset additional steel weight. By using the updated α values, the increase in EEDI for this ideal scenario is illustrated in Table 11.

Table 11: Estimation of EEDI accounting for additional increases in lightweight (α) due to machinery modifications and extra steel weight for ice strengthening, for fixed displacement.

Ice class	**IAS**	**IA**	**IB**	**IC**
ΔEEDI (%)	2.17 ± 0.40	1.64 ± 0.30	0.90 ± 0.16	0.03 ± 0.01

Table 11 shows an increase in the Attained EEDI compared to Table 7. This rise is attributed to the smaller denominator in Eq. 36 due to a higher α, reflecting increased lightweight from

ice strengthening and machinery changes. Even in an ideal scenario, these factors suggest a need for a greater capacity correction factor for higher ice classes.

3.2.2 Fixed Displacement with Dimensional Changes

Similar to Sec. 3.2.1, the fixed displacement scenario with dimensional changes is considered according to Eq. 27, incorporating changes in the MCR for the respective ice class. The calculation procedure follows the approach detailed in Sec. 3.1.2. The results are presented in Table 12.

Table 12: Estimation of the impact of additional weight from ice strengthening, and machinery modification on the dimensions and performance parameters of an equivalent open-water ship under fixed displacement constraints.

Ice Class	ΔL **(%)**	ΔC_b **(%)**	ΔS **(%)**	ΔP **(%)**
IAS	9.19 ± 1.48	-9.19 ± 1.48	4.31 ± 0.73	3.34 ± 0.56
IA	7.15 ± 1.33	-7.15 ± 1.33	3.27 ± 0.62	2.53 ± 0.48
IB	4.04 ± 0.47	-4.04 ± 0.47	1.78 ± 0.60	1.33 ± 0.10
IC	2.58 ± 0.53	-2.58 ± 0.53	1.14 ± 0.45	0.88 ± 0.34

Table 12 shows that dimensional changes are more pronounced for an equivalent open-water ship. For the IAS case (Table 8 and Table 12), comparing the scenario with only extra steel to the scenario with both extra steel and machinery weight, the length and block coefficient increase by about 35%, while the required power rises by approximately 39%. In contrast, the IC case shows only minor changes, which slightly reduce the attained values because of lower power requirements.

3.2.3 Fixed Deadweight with Increase in Length

Similar to Sec. 3.1.3, with a key adjustment involving the change in engine power output, which leads to an increase in machinery weight, as specified in Eq. 22. Consequently, the increase in length was calculated through iterative processes to achieve a balance between the hydrostatic equation and displacement based on weight, as detailed in Eq. 24. These findings are presented in Table 13.

Table 13: Estimation of the impact of additional weight from ice strengthening, and machinery modification on the dimensions and performance parameters of an equivalent open-water ship under fixed deadweight with constant C_b.

Ice Class	Increase in L (%)	Increase in P (%)
IAS	2.04 ± 0.51	1.82 ± 0.47
IA	1.53 ± 0.34	1.16 ± 0.32
IB	0.86 ± 0.21	0.62 ± 0.19
IC	0.45 ± 0.20	0.34 ± 0.18

Accounting for engine weight increases the calculated length relative to the case in which only steel weight is considered. The increase reaches 39% for IAS and 28% for IA. In contrast,

the effect is negligible for IB, while IC exhibits a reduction in length. These results indicate that the inclusion of machinery weight has a pronounced effect on higher ice classes, reflecting the substantially greater propulsion power required. In particular, IAS shows an increase of approximately 40%. The impact of these changes on the Attained EEDI of an equivalent ship is detailed in Table 14.

3.2.4 Fixed Deadweight with Increase in Length and Reduction in C_b

Similar to the approach used in the previous section, systematically reducing the block coefficient could also be explored to observe its effect on these outcomes.

Figure 9 indicates that increasing the MCR has a relatively minor influence on the resulting changes in length and power when compared to the baseline case shown in Figure 8. Considering both figures, the most extreme case (IAS with a 4% reduction in C_b) results in a power increase of approximately 16%, while the wetted surface area increases by about 19% when the machinery weight is included in addition to the steel weight. This indicates that the block coefficient strongly influences changes in length and power, especially when deadweight remains constant, and displacement varies. Variation in displacement mainly affects the wetted surface area, which in turn determines the required power increase.

3.2.5 Comparison of Attained EEDI

Identical to Sec. 3.1.5, EEDI changes resulting from alterations in power, deadweight, or both across all cases are detailed in Table 14, which is based on the calculation done in Secs. 3.2.1, 3.2.2, 3.2.3, and 3.2.4.

Table 14: Comparison of estimated EEDI under the effect of extra steel weight, and machinery modifications using fixed displacement, fixed deadweight, and the capacity correction factor mentioned by the regulations.

Ice Class	**IAS**	**IA**	**IB**	**IC**
Capacity Correction Factor (%)	2.07 ± 0.42	1.14 ± 0.17	0.82 ± 0.11	0.50 ± 0.10
EEDI ↑ (%) (Fixed DWT with L↑)	1.55 ± 0.47	0.98 ± 0.32	0.53 ± 0.19	0.29 ± 0.18
EEDI ↑ (%) (Fixed Δ)	2.17 ± 0.40	1.64 ± 0.30	0.90 ± 0.16	0.03 ± 0.01
EEDI ↑ (%) Fixed DWT with L↑, $C_b(4\%)$ ↓	3.39 ± 0.66	2.99 ± 0.49	2.43 ± 0.30	2.14 ± 0.25
EEDI ↑ (%) (Fixed Δ with L↑, C_b ↓)	5.56 ± 0.89	4.19 ± 0.53	2.28 ± 0.36	0.94 ± 0.25

As with Table 10, correction factors reported in the literature (Table 3) were derived using ship data with specific deadweight from Table 15. However, when considering machinery weight changes in addition to extra steel weight, the increase in EEDI exceeds what the correction factors suggest, as displayed in Table 14. This is except for the fixed deadweight scenario with increased length, which still underestimates the correction factors. In the ideal scenario,

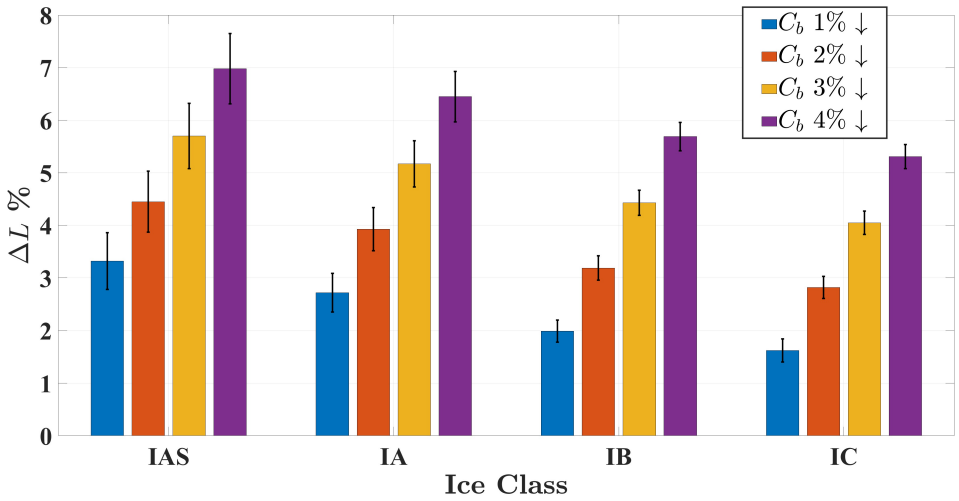

(a) Increase in Length

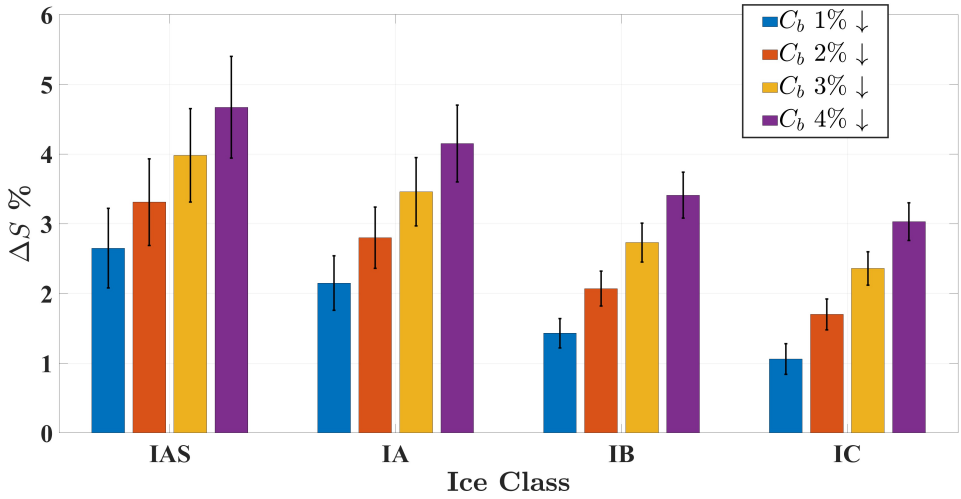

(b) Increase in Wetted Surface Area

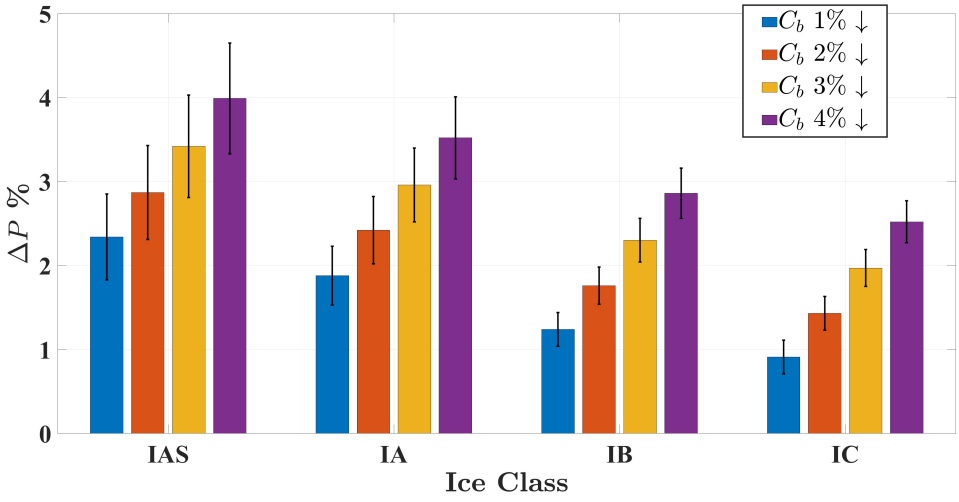

(c) Increase in Power

Figure 9: Estimation of the impact of additional weight from ice strengthening, and machinery modification on the dimensions and performance parameters of an equivalent open-water ship under fixed deadweight with various C_b.

without dimensional changes, values indicate potential improvement of correction factors when accounting for heightened engine weight, with only minor changes for the ice class IC. For the equivalent ship with fixed displacement and dimensional changes, a capacity correction factor increase of approximately 1.8 to 3.2 times is necessary, from the lowest to the highest ice classes. Similarly, an equivalent ship with fixed deadweight exhibits more change relative to the base capacity correction factor, but not as drastically as the fixed displacement method.

3.3 Minimum Engine Power

The relationship between ice-class requirements and EEDI compliance reveals a fundamental conflict between operational capability and environmental regulations. The study by Saisto [44] demonstrates this discrepancy for tanker vessels, where the power required by the Finnish–Swedish Ice Class Rules (FSICR) for Ice Class 1A Super (7490 kW) significantly exceeds the power permitted under EEDI regulations (4096–4432 kW). This highlights a substantial gap between the propulsion demand for safe ice navigation and the limits imposed by emission regulations.

Similarly, Lu et al. [30] investigated the influence of bow design and ice class on EEDI compliance. Their results show that lower ice classes, such as IC, can satisfy EEDI requirements across all bow configurations, whereas higher ice classes, particularly IAS, fail to meet future EEDI limits regardless of design variations. Intermediate classes (IB and IA) exhibit conditional compliance depending on hull form and optimization measures implemented.

These findings collectively indicate that the propulsion power required for high ice-class performance often exceeds the allowable limits defined by EEDI, creating a critical design trade-off. Consequently, ice-going vessels must be designed to operate with the minimum propulsion power that still satisfies ice-class requirements [29].

3.4 Effect of Thicker Propeller Blade

Open-water and icegoing propellers differ significantly in their design philosophy due to operating environments and load conditions. Open-water propellers are optimized for maximum hydrodynamic efficiency in steady, ice-free conditions, following standards such as IMO and ISO. They typically feature thin, highly skewed blades with sharp leading edges to minimize cavitation and vibration, commonly made from Nickel-Aluminum Bronze for good strength and corrosion resistance [10].

In contrast, ice-going propellers are designed to balance efficiency, strength, and impact resistance, operating in environments containing brash ice and occasional direct ice impacts. An optimization study, [45] found that ice strengthening necessitates a substantial increase in propeller thickness, approximately 40% greater than conventional open-water designs that did not fully account for off-design ice conditions, which reduced the efficiency. In a numerical study [42], simulations revealed that the blade root experiences sustained high stress, necessitating sufficient thickness to withstand continuous loading. The blade tip undergoes periodic impacts and localized plastic deformation. Under extreme conditions, ice-milling loads exceeded standard hydrodynamic loads by more than 2.5 times, directly influencing the required torque, thrust, and power capacity of the main engine.

Their design follows ice-class regulations such as the Finnish–Swedish Ice Class Rules [9] which account for both hydrodynamic and impulsive loads. These propellers feature thicker blades, rounded or reinforced leading edges, and larger hubs to resist ice-induced stresses and fatigue, which effects are investigated by various researchers.

To compare open-water propeller designs with ice-strengthened propellers for classes IC, IB, IA, and IAS on a single-screw bulk carrier and a twin-screw RoRo/ferry was considered by [44]. They investigated the effect of the FSICR on propeller efficiency by incorporating relevant correction factors for the EEDI of ice-class vessels. Since this study focuses on bulk carriers, results showed that ice strengthening significantly increased propeller blade thickness—particularly between 0.25R and 0.5R—with thickness rising proportionally to various ice classes (up to 230% for IAS at 0.4R on the bulk carrier). This added thickness and associated drag reduced propeller efficiency and increased required delivered power, with penalties ranging from 2.8% (IC/IB) to 4.3% (IAS) for the bulk carrier.

Moreover, [47] found that the strength requirements and increased blade thickness of ice-class propellers constrain the use of conventional hydrodynamic sections. As a result, blunter blade profiles optimized for ice milling are adopted, prioritizing strength over cavitation performance. Each 10% thickness increase reduces efficiency by 0.6–0.8%. Conventional cavitation-reducing measures, such as skew (limited to 5–10°) and tip unloading, are largely restricted by ice-strength considerations. Consequently, ice propellers operate at about 1.5 times higher loading than open-water designs and are often overdesigned to prevent cavitation, causing efficiency losses of 2–2.5%.

In another scenario [46] figured that polar ship propellers, operating under high load to overcome ice resistance, are prone to cavitation. Also, ice blockage reduces inflow speed, increasing thrust and torque, but severe cavitation diminishes this effect. In ice blockage tests, cavitation reduced open-water efficiency by about 2% and weakened the influence of ice blockage on thrust and torque.

3.5 Effect energy saving technologies [f_m]

In open-water ships, energy-saving devices include bulbous bows, air lubrication systems, and wind-assisted propulsion like sails, which are unsuited for ice-going vessels due to ice-breaking needs. Solar panels are less effective in icy regions with low sunlight and potential ice coverage. Additionally, advanced hull coatings preventing biofouling and waterjets optimized for speed face challenges in ice. These technologies require adaptations to function amidst ice and extreme cold conditions.

A MEPC [20] study found that ships meeting Phase 1 EEDI requirements often use energy-saving devices (ESD), like pre-swirl stators and nozzles, reducing propulsion power by 4% to 6%. However, such technology is rarely used in ice-classed ships due to ice-related damage risks. Consequently, a 5% margin from reference lines was proposed for ice-classed ships. Further discussions led to defining this margin for high ice class ships (IA Super and IA) via a new correction factor, incorporated into EEDI guidelines by resolution MEPC.322(74) [20] that is defined in Eq. 38.

$$f_m = 1.05 \tag{38}$$

Among the various technologies, we focus on the impact of the bow shape on power requirements across different ship types. Bulbous bows and icebreaking bows serve distinct design purposes. Bulbous bows enhance open-water efficiency by reducing wave resistance, while icebreaking bows prioritize structural strength and ice-clearing, using steep stems, flares, and downward-sloping profiles to fracture ice effectively. Below are the detailed differences between these designs. Eventually, an optimized bow design with a moderate ice capability is key to balancing ice performance with energy efficiency, especially when the total energy consumption of both the merchant ship and the assisting icebreaker is considered [29].

3.5.1 Bulbous bow

Bulbous bows are designed to minimize wave-making resistance at a vessel's optimal design speed and draught by generating a counter-wave that partially cancels the ship's natural bow wave. This interaction can enhance fuel efficiency by up to 12–15% in large vessels and significantly reduce required engine power. However, their effectiveness depends on speed and draught, often optimized for a specific Froude number—and can decrease at lower speeds due to increased viscous drag [36].

The bow form is a critical parameter in ship design, influencing hydrodynamic resistance as well as structural and operational performance. Besides improving propulsion efficiency, a well-designed bow contributes to collision protection, accommodates bow thrusters, increases forward buoyancy or ballast capacity, and mitigates pitch motion. In ice-strengthened bows, designed for durability in ice-covered waters, open-water resistance is typically higher, reducing fuel efficiency.

Dihedral bulbous bows substantially reduce calm-water resistance in displacement hulls by approximately 15–20% and in semi-displacement hulls by 10–12%, primarily through smoother pressure distribution and lower bow wave formation [35]. This effect is illustrated in Fig. 10, which compares the bow wave patterns of the same vessel with and without a bulbous bow. Similarly, Le et al. [37] reported that optimized bulb geometries can reduce added wave resistance by up to 48% and total resistance by 13% at a Froude number of 0.163. In calm-water conditions, resistance reductions of about 6% were observed even for bulbs with larger wetted surface areas.

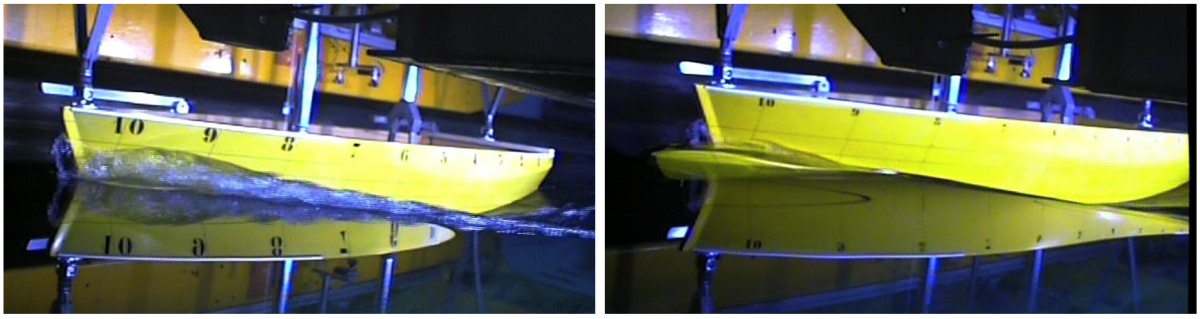

Figure 10: Comparison of bow wave patterns for a vessel with and without a bulbous bow at $F_r = 0.33$, demonstrating the reduction in wave-making resistance [35].

3.5.2 Ice Going bow

When a ship advances into an intact ice field, ice breakage occurs primarily along the waterline, where the hull directly contacts the ice cover. In this region, the hull surface acts as a rigid boundary during icebreaking. As the ship progresses, individual ice wedges detach from the unbroken sheet at the contact zones. The presence of a bulbous bow can increase ice resistance by approximately 11%, due to additional buckling and bending induced during ice–ship interaction [34]. The buttock angle and the first sub-region of the bow are critical for icebreaking performance. Resistance increases with larger buttock angles and decreases with higher waterline angles, whereas ice pressure exhibits the opposite trends [40].

4 Discussion

This research investigates the effects of ice-class requirements on the performance of ships navigating open waters, with particular focus on changes in capacity, minimum power requirements, and the integration of energy-saving technologies. Employing a hybrid approach, the study combines a thorough literature review with original computational analyses to deliver comprehensive insights into the subject matter.

According to the literature, ice-going vessels are equipped with additional steel for hull reinforcement and more powerful engines to navigate icy conditions. Compensating for variations due to changes in capacity and ice strengthening requires adjustments ranging from 0.50% to 2.07% across different ice classes. These modifications were systematically applied to equivalent open-water ships using two distinct methodologies: fixed deadweight and fixed displacement, both with and without dimensional changes.

The fixed deadweight method for an equivalent ship estimates EEDI increases primarily based on power gains from length extension, initially underestimating the correction factor. Even with additional engine weight, the figures remained below recommended values. To address this, a systematic reduction in block coefficient was applied and compared with rule-based correction factors. The results show that this approach leads to a higher Attained EEDI, indicating a more pronounced impact on ship performance. For Ice Class IC, the Attained EEDI increases by approximately 2.20% when considering both steel weight alone and the combined effect of steel and machinery. This increase is nearly four times higher than the 0.5% predicted by rule-based corrections. For higher ice classes, the effect becomes significantly more pronounced. In the case of IAS, the Attained EEDI increases by approximately 42% when only the additional steel weight is considered, and a further 22% increase is observed when machinery weight is also included from the values suggested by regulations. This trend persisted when factoring in engine weight, though the impact remained relatively minor.

The fixed displacement method can be viewed in two ways. First, with no dimensional change, where an open-water ship is equipped with extra steel and experiences an equal reduction in capacity. Initially, when the lightweight increase was due to extra steel alone, the EEDI increase aligned with correction factors for IB and IC but underestimated IAS and overestimated IA. However, when engine weight changes were considered, it revealed that correction factors were actually lower than the calculated outcomes for all cases except IC. The selected ships possess higher engine power than IC requires, necessitating a reduced MCR to meet requirements, which cancels the extra weight of steel. Second, when dimensional changes are used to represent an equivalent ship, considering only the additional steel weight leads to higher Attained EEDI values compared to regulatory estimates. In this case, the Attained EEDI approximately doubles for IAS and triples for IC relative to the values prescribed by the regulations. When the effect of machinery weight is also included, the trends differ between ice classes. For IAS, the Attained EEDI increases by a further 41% compared to the steel-only case, reflecting the substantial impact of increased engine power. In contrast, for IC, the correction is reduced by approximately 39% relative to the previous case, as the lower machinery weight partially offsets the effect of additional steel. Eventually, this analysis suggests that when changes are assessed under fixed deadweight conditions, the increase in EEDI is less pronounced, given that a key parameter, deadweight, remains fixed, stabilizing the calculation basis. Secondly, for equivalent ships, structural modifications due to ice strengthening can significantly alter hull shapes, thereby drastically affecting vessel performance, particularly in terms of energy efficiency and hydrodynamic characteristics.

Considering the various scenarios discussed, the additional weight from steel and engine

modifications can lead to substantial changes in the ship's hull form, notably affecting its length and block coefficient compared to an equivalent open-water design. Consequently, Attained EEDI will increase, indicating that there is significant scope for improving correction factors. These changes are particularly pronounced in smaller ships with limited capacity, where variations in lightweight can have a greater impact, as is often observed in vessels operating in the Baltic Sea.

Moreover, navigating icy waters necessitates specific regulatory compliance, resulting in major differences between FSICR power requirements and EEDI regulations for tankers. Ice-class ships require more robust engines and thicker propeller blades, up to 40% thicker, to withstand ice stresses, which decreases hydrodynamic efficiency and raises power demands, increasing power requirements by 2.8% to 4.3%. Bulbous bows enhance open-water ship efficiency by reducing wave resistance and improving fuel consumption by 12-15%, yet are less effective in icy conditions, where icebreaking bows counter ice but increase resistance. Overall, ice-going ships need more power, have reduced capacity, and face challenges in integrating eco-friendly technologies due to their unique structural requirements and operational constraints.

5 Conclusion

This study examined the impact of ice-class requirements on ship performance in open-water conditions, focusing on capacity, power demand, and energy efficiency. The results show that structural reinforcement and increased engine requirements lead to higher Attained EEDI, with the magnitude depending strongly on the chosen equivalence method. While fixed deadweight scenarios show limited increases, fixed displacement cases, especially with dimensional changes, result in significantly higher deviations due to altered hull forms. The findings also indicate that current correction factors may not adequately reflect the resulting EEDI increase, particularly for smaller vessels. Additionally, propulsion and design constraints in ice conditions further reduce efficiency and limit the applicability of energy-saving technologies. The basis of this investigation is on simplified assumptions for only bulk carriers and does not fully capture real operational and environmental variability. Further investigation could consider other ship types and explore experimental validation of the hypothetical equivalent ships examined in this study.

References

[1] Finnish Shipowners' Association, *Key Figures of Maritime Transport in Finland*, 2024. Available: https://shipowners.fi/en/competitiveness/key-figures-of-maritime-in-finland/

[2] International Maritime Organization, *Resolution MEPC.203(62): Amendments to MARPOL Annex VI (Inclusion of Regulations on Energy Efficiency for Ships in MARPOL Annex VI)*, 2011.

[3] International Maritime Organization, *Resolution MEPC.328(76): Amendments to the Annex of the Protocol of 1997 to Amend the International Convention for the Prevention of Pollution from Ships, 1973, as Modified by the Protocol of 1978 Relating Thereto (2021 Revised MARPOL Annex VI)*, 2021.

[4] International Maritime Organization, *Resolution MEPC.231(65): 2013 Guidelines for Calculation of Reference Lines for Use with the Energy Efficiency Design Index (EEDI)*, 2013.

[5] International Maritime Organization, *MEPC 62/6/4: Calculation of Parameters for Determination of EEDI Reference Values*, 2011.

[6] ClassNK, *Outlines of EEXI Regulation* [PowerPoint presentation], Accessed: Aug. 08, 2024. [Online]. Available: https://www.classnk.or.jp/hp/pdf/activities/statutory/eexi/eexi_rev3e.pdf

[7] International Maritime Organization (IMO), *MEPC 74/7/2, Energy Efficiency Improvement Measure for Existing Ships*, 2019.

[8] International Maritime Organization (IMO), *Resolution MEPC.350(78), 2022 Guidelines on the Method of Calculation of the Attained Energy Efficiency Existing Ship Index (EEXI)*, 2022.

[9] Finnish–Swedish Ice Class Rules (FSICR), *Traficom Publication 200/01/2019*, Finnish Transport and Communications Agency (Traficom), 2019.

[10] J. P. Breslin and P. Andersen, *Hydrodynamics of Ship Propellers*, Cambridge University Press, 1996.

[11] International Maritime Organization (IMO), *Circular MEPC.1/Circ.896, 2021 Guidance on Treatment of Innovative Energy Efficiency Technologies for Calculation and Verification of the Attained EEDI and EEXI*, 2022.

[12] International Maritime Organization (IMO), *The International Convention for the Prevention of Pollution from Ships, 1973, as Modified by the Protocol of 1978 (MARPOL 73/78), Consolidated Edition*, International Maritime Organization, 2022.

[13] L. Blasig, *Optimisation of the hull steel weight considering ice class for the design of an electric ferry*, Master's thesis, Nordic Master Programme in Maritime Engineering, Aalto University, 2024. Available: https://urn.fi/URN:NBN:fi:aalto-202409016105

[14] Aker Arctic Technology Inc., *EEDI Study of Capacity Correction Factors for Finnish-Swedish Ice Classes for Trafi (Report)*, 2017.

[15] MEPC 71/5/6, *Proposal for Amendments to the 2014 Guidelines on the Method of Calculation of the Attained Energy Efficiency Design Index (EEDI) for New Ships - New Ice Class Correction Factors for Capacity*, 2017.

[16] T. Mattson, *PREEDICT – EEDI Power Correction Factors fj for Ice Class Ships*, Winter Navigation Research Board Report No. 105, Helsinki and Norrköping, 2018.

[17] T. Avellan, *Weight estimation of ice strengthened hull structures*, Master's thesis, Nordic Master's Programme in Cold Climate Engineering, Aalto University, 2020. Available: https://urn.fi/URN:NBN:fi:aalto-2020122056315

[18] I. Mazanikov, *Impact of Energy Efficiency Regulations on Ships Operating in Ice*, Master's thesis, Master's Programme in Mechanical Engineering, 2025.

[19] K. Riska, *Ship-Ice Interaction in Ship Design: Theory and Practice*, 2019. Available: https://pdfs.semanticscholar.org/c14d/add4eb6da9e68e5f4be4ff6c18acbd90a742.pdf

[20] IMO, *MEPC 71/5/2, "Implementation of Energy Efficiency Design Index for Ice Class Ships"*, Marine Environment Protection Committee, International Maritime Organization, 2017.

[21] H. Schneekluth and V. Bertram, *Ship Design for Efficiency and Economy*, 2nd ed., Butterworth-Heinemann, 1998. Available: https://doi.org/10.1016/B978-0-7506-4133-3.X5000-2

[22] J. Alanko, *Laivan yleissuunnittelu*, Turku, Finland: Karhukopio, 2007.

[23] L. Larsson and H. C. Raven, edited by J. R. Paulling, *Ship Resistance and Flow*, Jersey City, N.J.: Society of Naval Architects and Marine Engineers, 2010.

[24] L. Thomas, *Ship Design and Construction*, The Society of Naval Architects and Marine Engineers (SNAME), USA, 2003. ISBN: 0939773406

[25] International Towing Tank Conference (ITTC), *Recommended Procedures and Guidelines — 1957 ITTC Model-Ship Correlation Line for Frictional Resistance*, Presented at the 10th ITTC, 1957.

[26] Murray, R., *Ship Design and Construction*, Society of Naval Architects and Marine Engineers, New York, 1965.

[27] International Maritime Organization (IMO)—GreenVoyage2050, *Energy Efficiency Technologies Information Portal*, n.d. Accessed [insert date of access]. Available at: https://www.reddit.com/r/PlaystationPortal/comments/1lppe23/how_does_the_portal_work/.

[28] Det Norske Veritas (DNV), *Rules for the Classification and Construction of Steel Ships*, Oslo, Norway, 1972.

[29] Riska, K., *Energy Efficiency of the Baltic Winter Navigation System*, Winter Navigation Research Board, Research Report No. 83, Finnish Transport Safety Agency, Swedish Maritime Administration, Finnish Transport Agency, Swedish Transport Agency, Finland–Sweden, 2015. ISSN 2342-4303, ISBN 978-952-311-032-8. Available at: https://www.traficom.fi/sites/default/files/media/file/W17-4%20ICEEDI.pdf.

[30] Lu, Y., Gu, Z., Liu, S., Wu, C., Shao, W., & Li, C., *Research on Main Engine Power of Transport Ship with Different Bows in Ice Area According to EEDI Regulation*, *Journal of Marine Science and Engineering*, 2021, 9(11), 1241. https://doi.org/10.3390/jmse9111241.

[31] D. G. M. Watson and A. W. Gilfillan, *Some Ship Design Methods*, Transactions of the Royal Institution of Naval Architects (RINA), vol. 119, 1977.

[32] Harvald, S. A., and Jensen, P. J., *Resistance and Propulsion of Ships*, Koehler Publishers, Copenhagen, 1992.

[33] K. J. Rawson and E. C. Tupper, *Basic Ship Theory, Vol. 1: Hydrostatics and Stability*, 5th ed., Butterworth-Heinemann, 2001.

[34] Afrizal, A., "Effect of Bulbous Bow on Ice Resistance of Ice Ship," *Proceedings of the International Conference on Naval Architecture and Ocean Engineering*, 2018. .

[35] Díaz-Ojeda, H.R., Pérez-Arribas, F., & Turnock, S.R., *The influence of dihedral bulbous bows on the resistance of small fishing vessels: A numerical study*, *Ocean Engineering*, 2023, **281**, 114661. https://doi.org/10.1016/j.oceaneng.2023.114661.

[36] Way, H. F. M., Hudson, D., & Turnock, S. R., "Assessment of Bulbous Bow Performance Over Operational Profiles Using Full Scale Data," in *Proceedings of the Full Scale Ship Performance Conference*, London, UK, 24–25 October 2018, The Royal Institution of Naval Architects, 2018.

[37] Le, T.-K., He, N. V., Hien, N. V., & Bui, N.-T., "Effects of a Bulbous Bow Shape on Added Resistance Acting on the Hull of a Ship in Regular Head Wave," *Journal of Marine Science and Engineering*, vol. 9, no. 6, p. 559, 2021. https://doi.org/10.3390/jmse9060559.

[38] Lap, A. J. W., "Diagrams for determining the resistance of single-screw ships," *International Shipbuilding Progress*, p. 179, 1954.

[39] Sun, X., and Huang, X., "Ice resistance of a naval ship with a non-icebreaking bow," *Journal of Marine Science and Engineering*, vol. 11, no. 7, 2023, Art. no. 1380. doi:10.3390/jmse11071380.

[40] Zhu, L., Xue, Y., Guo, R., Zan, Y., Lu, Y., & Zhang, Y., "A Multi-objective Optimization Method for Resistance Performance of an Icebreaker Bow Based on Fully Parameterized Modeling," *Journal of Marine Science and Application*, 2025. DOI: https://doi.org/10.1007/s11804-025-00629-0

[41] Riska, K., "Design of Ice Breaking Ships," in *Encyclopedia of Life Support Systems (EOLSS)*, UNESCO-EOLSS, 2018. .

[42] Yuan, X., Wang, X., Xiong, W., Xue, M.-A., & Wang, Y., *Prediction of propeller loads and structural response induced by ice-propeller milling in a mixed ice-water environment*, College of Harbour, Coastal and Offshore Engineering, Hohai University, Nanjing, China.

[43] Lu, Q., Zhang, J., Wang, K., and Li, M., "Scenario-based optimization design of icebreaking bow for polar navigation," *Cold Regions Science and Technology*, vol. 198, 2022, Art. no. 103571. doi:10.1016/j.coldregions.2022.103571.

[44] Saisto, I., & Turunen, T., *Effect of the FSICR to Propeller Efficiency*. Winter Navigation Research Board, Research Report No. 108, Finnish Transport Infrastructure Agency, and Swedish Transport Agency, Helsinki and Norrköping, 2020. ISSN 2342-4303, ISBN 978-952-311-491-3.

[45] Gu, C., Han, K., Weng, K., Wang, C., & Wang, C., *Design Method for Low-Ice-Class Propellers Based on Multi-Objective Optimization*, *Journal of Marine Science and Engineering*, 2024, 12(11), 1986. https://doi.org/10.3390/jmse12111986

[46] Zhou, L., Zheng, S., Diao, F., Ding, S., & Gao, J., *Experimental and Numerical Study on Ice Blockage Performance of Propeller in Cavitation Flow*, *Water*, 2022, 14(7), 1060. https://doi.org/10.3390/w14071060

[47] Pustoshny, A. V., Darchiev, G. K., & Frolova, I. G., *The Problem of Propeller Design for High Ice Class Transportation Ships*, *Proceedings of the Fifth International Symposium on Marine Propulsors (smp'17)*, Espoo, Finland, June 2017. Krylov State Research Centre, St. Petersburg, Russia.

Appendix

Table 15: Selected bulk carriers with corresponding data on principal dimensions, lightweight, deadweight, and engine power.

Bulk carrier	L_{oa} **[m]**	**B [m]**	**T [m]**	**D [m]**	**DWT [ton]**	**LWT [ton]**	**MCR [kW]**
Bulk carrier	110.0	21.0	3.9	7.9	5159.0	2343.0	2400.0
Bulk carrier	130.0	24.0	6.5	10.0	11000.0	4299.0	5100.0
Bulk carrier	170.7	27.0	9.7	13.8	29721.0	6159.0	6156.0
Bulk carrier	171.9	28.0	10.6	15.0	30850.0	6349.0	7056.0
Bulk carrier	175.0	26.1	10.1	13.9	28588.0	7352.0	5847.0
Bulk carrier	179.9	28.4	10.0	14.1	31630.0	9459.0	5508.0
Bulk carrier	180.0	30.0	10.1	14.7	34613.0	10396.0	7900.0
Bulk carrier	181.1	30.0	9.8	14.6	33470.0	8530.0	7293.0
Bulk carrier	186.4	27.8	9.8	15.6	31800.0	8113.0	6681.0
Bulk carrier	189.9	32.3	10.8	17.1	45108.0	8470.0	8730.0
Bulk carrier	190.0	32.3	12.5	17.2	53208.0	10280.0	9480.0
Bulk carrier	192.3	32.3	11.0	15.7	49300.0	10865.0	8670.0
Bulk carrier	197.1	32.3	11.0	15.7	45161.0	10270.0	11620.0
Bulk carrier	199.9	32.3	11.0	19.3	47171.0	13065.0	9960.0
Bulk carrier	200.0	32.3	11.3	18.5	50850.0	11621.0	8300.0
Bulk carrier	224.8	32.3	13.8	20.1	72335.0	10627.0	8253.0
Bulk carrier	224.9	32.3	14.4	20.1	82356.0	10962.0	9378.0
Bulk carrier	225.0	32.3	13.9	19.2	73281.0	9965.0	8878.0
Bulk carrier	225.5	23.8	8.1	14.8	23000.0	8707.0	7750.0
Bulk carrier	225.6	23.7	11.5	15.0	37300.0	11000.0	7200.0
Bulk carrier	229.0	32.3	14.5	20.2	81874.3	13504.0	10170.0
Bulk carrier	229.0	32.3	14.6	20.2	81272.0	13714.0	8351.8
Bulk carrier	249.9	43.0	14.5	21.3	109221.0	15820.0	12900.0
Bulk carrier	288.9	45.1	16.5	24.7	150888.0	22766.0	14320.0
Bulk carrier	289.0	45.0	16.5	24.3	155200.0	25145.0	18736.0
Bulk carrier	289.0	45.0	16.5	24.3	158800.0	26415.0	18660.0
Bulk carrier	291.7	48.0	17.1	23.7	171882.0	26176.0	19669.0
Bulk carrier	292.0	45.0	16.5	24.0	157500.0	26410.0	15861.0
Bulk carrier	292.0	45.0	16.5	24.8	158800.0	47000.0	18660.0